

Aus dem Universitätsklinikum Münster  
Klinik für Schlafmedizin und neuromuskuläre Erkrankungen  
Direktor: Univ.-Prof. Dr. med. P. Young

**The effect of granulocyte colony-stimulating factor on the  
peripheral nerve and the progress of Charcot-Marie-Tooth  
neuropathy type 1A in a rat model**

INAUGURAL - DISSERTATION

zur  
Erlangung des Doctor medicinae

der Medizinischen Fakultät  
der Westfälischen Wilhelms-Universität Münster

Vorgelegt von Van Cauwenberge Margot G.A.  
aus Wetteren, Belgien  
2016

Gedruckt mit Genehmigung der Medizinischen Fakultät der Westfälischen Wilhelms-Universität Münster

Dekan: Prof. Dr. M. Herrmann

1. Berichterstatter: Univ.-Prof. Dr. med. P. Young

2. Berichterstatter: Prof. Dr. V. Shahin

Tag der mündlichen Prüfung: 15.12.2016

Aus dem Universitätsklinikum Münster  
Klinik für Schlafmedizin und neuromuskuläre Erkrankungen  
Direktor: Univ.-Prof. Dr. med. P. Young  
Referent: Univ.-Prof. Dr. med. P. Young  
Koreferent: Prof. Dr. rer. nat. V. Shahin

## ZUSAMMENFASSUNG

The effect of granulocyte colony-stimulating factor on the peripheral nerve and the progress of Charcot-Marie-Tooth neuropathy type 1A in a rat model

Van Cauwenberge, Margot

Morbus Charcot Marie Tooth (CMT) ist die Sammelbezeichnung für eine Gruppe von genetische chronisch progrediente Neuropathien mit variabler distalen Muskelschwäche und Sensibilitätsstörungen. Aktuell bestehen keine kausale Therapieoptionen für die CMT . CMT1A ist die häufigste Subtyp. In 90% dieser Patienten ist der verantwortliche Defekt die Duplikation des Gens für das periphere Myelinprotein 22 (PMP22).

Von Granulocyte colony-stimulating factor (G-CSF) sind letzgens neuroprotektive Qualitäten in Hirnneuronen nachgewiesen. In dieser Arbeit wurde das therapeutische potentiell von G-CSF untersucht für die Behandlung von Morbus Charcot Marie Tooth in einem Tiermodel für CMT1A. PMP22<sup>+++</sup> transgene CMT1A Ratten (33) und wild-Typen (17) werden random mit G-CSF (10, 50, 100 µg/kg/tgl. subkutan) oder Placebo behandelt ab den 15 bis 30 Lebenstag. Auskünfte waren die nerve conduction velocity (NCV) und compound muscle action potential (CMAP) in den Nervus caudalis und Myelination (G-Ratio), axonale Erhaltung, Vaskularisation und zelluläre Immunreaktion in den Nervus ischiadicus und tibialis.

Es wurden keine signifikanten Unterschiede festgestellt in die NCV, CMAP oder in die Myelination, axonale Erhaltung und Immunreaktion zwischen peripheren Nerven von Tieren behandelt mit G-CSF oder Placebo. Eine zugenommen Nervendurchmesser und Zunahme der Zahl an endoneuralen Blutgefäße wurde nachgewiesen in den PMP22 transgene Ratten.

Aktenzeichen tierexp. Genehmigung 8.87-51.04.20.09.347 durch das Landesamt für Natur, Umwelt und Verbraucherschutz Nordrhein-Westfalen am 17.08.2009

Tag der mündlichen Prüfung: 15.12.2016

## ERKLÄRUNG

Ich gebe hiermit die Erklärung ab, dass ich die Dissertation mit dem Titel:

The effect of granulocyte colony-stimulating factor on the peripheral nerve and the progress of Charcot-Marie-Tooth neuropathy type 1 in a rat model

in der Klinik für Schlafmedizin und neuromuskuläre Erkrankungen

unter der Anleitung von: Univ- Prof. Dr. med. P. Young

1. selbständig angefertigt,
2. nur unter Benutzung der im Literaturverzeichnis angegebenen Arbeiten angefertigt und sonst kein anderes gedrucktes oder ungedrucktes Material verwendet,
3. keine unerlaubte fremde Hilfe in Anspruch genommen,
4. sie weder in der gegenwärtigen noch in einer anderen Fassung einer in- oder ausländischen Fakultät als Dissertation, Semesterarbeit, Prüfungsarbeit, oder zur Erlangung eines akademischen Grades, vorgelegt habe.

Aachen, 28 Januar 2016

Ort, Datum

Preface .....	1
Introduction – Background .....	2
Research goals.....	6
Materials and methods.....	7
Results.....	11
Subjects .....	11
Electrophysiology .....	13
Nerve Histology .....	15
<i>Sciatic nerve histology</i> .....	15
<i>Tibial nerve histology</i> .....	21
<i>Nerve vascularization following G-CSF</i> .....	24
<i>The immune system: role in early CMT?</i> .....	31
Discussion.....	32
No place for G-CSF in the treatment of CMT? .....	32
G-CSF and the immune response .....	36
G-CSF and angiogenesis.....	37
At least some new findings .....	37
G-CSF for CMT: end of story? .....	38
Conclusions and perspectives for further research.....	40
References.....	42
Curriculum Vitae .....	48

## **Preface**

This paper is the result of an interesting research period that brought me insight and valuable skills in the domain of neurogenetics. It would not have been possible without the contributions of the following persons, that I would like to thank:

First of all I would like to thank promotor Prof. Dr. Peter Young, for providing me the opportunity to discover experimental research and bringing the subject of Charcot-Marie-Tooth disease to my interest. Thanks also to co-promoters Dr. Burkhard Gess and Dr. Ilka Kleffner for their practical guidance and advice in carrying out the study.

I would like to express my very special thanks to Dominik Röhr, for his ever-kind assistance with many big and little things in the laboratory. His never fading enthusiasm and devotion to help was highly appreciated and made an important contribution to this work.

Special thanks also to Joke Nowitzki, for introducing me into the world of nerve histology and “enlighten” the work at the microtome.

I would like to thank Brigit Geng for the help in hematological analysis and sharing experience with the administration of G-CSF.

Finally, I would like to thank the nursing staff of the animal housing facility for their help and creativity in managing our therapy protocols in the breeding room.

To mama and Anna for their love and support.

## Introduction – Background

Charcot Marie Tooth disease (CMT) refers to a group of hereditary neuropathies characterized by variable distal muscle weakness and sensory loss (Dyck et al, 2005; Klein, 2007). It is named after Charcot, Marie and Tooth, who first described the disease in 1886. The more descriptive term “hereditary motor and sensory neuropathy” (HMSN) is used as well. The prevalence of CMT is estimated at 2 to 4 per 10.000 persons in European countries (Martyn et al., 1997).

The CMT neuropathies are divided in multiple subtypes that differ in clinical course, pathophysiology and genetics. The primary classification is based on the relative extend of axonal and demyelinating pathology in disease pathogenesis, with CMT subtypes 1,4,5 and 6 being primarily a demyelinating pathology with reduced nerve conduction velocity (NCV, <38 m/s), and CMT 2 being principally an axonal pathology with preserved or mildly slowed NCV (>38 m/s) (Pareyson et al., 2009). Further subclassification of CMT is derived from specific pathogenic genetic alterations, that have been identified in already more than thirty different gene loci. The most common genetic alterations involve genes coding for the peripheral myelin protein 22 (PMP22), myelin protein zero (MPZ) and the gap-junction protein connexin 32 (Cx32, also called “gap junction protein beta 1” (GJB1). (Klein, 2007; see <http://www.molgen.ua.ac.be/cmtmutations>).

The most frequent CMT subtype is CMT1A, accounting for 40-50% of all CMT patients (Martyn et al., 1997). In 90% of these patients, the responsible defect is a duplication of a 1.5 Mbp region on chromosome 17p11.2-12, that includes the gene for peripheral myelin protein 22 (PMP22) (Lupski et al.,1991). This small four-domain membrane protein is found in the compact myelin of Schwann cells and is thought to stabilize myelin (Kamholz et al., 2000). Duplication of the PMP22 gene leads to hypo- and demyelination via a gene-dosage dependent toxic gain of function, but the precise pathophysiology remains unknown (Sutter et al., 2003). In rare cases (1%), CMT1A is caused by point mutations in the PMP22 gene. Patients with heterozygosity for the PMP22 duplication demonstrate segmental demyelination in both peripheral sensory and motor nerves. As a result, NCV's are reduced below 38 m/s before the onset of clinical signs. Ensuing axonal damage leads to a peripheral symmetric sensorimotor neuropathy, with slow progression from distal to proximal limb muscles. The clinical picture shows large variability but typically starts between 10 to 20 years of age with

moderate weakness and muscle atrophy of the intrinsic foot muscles leading to hammer toes, pes cavus or planus deformation. Moderate sensory loss in the feet and later hands are present in early disease stage. Proximal progression involves the peroneal and calf muscles in the lower limb as well as upper limb muscles, with reduction to loss of deep tendon reflexes. As skeletal deformations start to develop, musculoskeletal pain may occur. Walking difficulties and steppage gait often develop in later disease stage, but an evolution to wheelchair dependency is seldom (Pareyson et al., 2009; Dyck et al., 2005; Shy, 2004; Hattori et al., 2003). The disease does not affect life expectancy, but has a high impact on life quality due to impaired mobility, reduced fine motor hand function and musculoskeletal or neuropathic pain.

There is to date no causal therapy for any subtype of CMT (Young et al., 2008). Current support is multidisciplinary and consists of physical therapy, lifestyle advice, orthopedic devices and surgery for skeletal deformities. Past research aimed to identify substances that could improve the function, survival or interaction of axons and/or Schwann cells, both by direct and indirect influences on the genetic defect in CMT patients.

The neurotrophic factor Neurotrophin 3, a component of the Schwann cell autocrine survival regulation, was proven to favor axonal regeneration and sensory loss in a study of CMT1A-xenograft harboring mice and Trembler(J) mice with a peripheral myelin protein 22-point mutation, as well as a small placebo-controlled pilot sample of human CMT1A patients (n=8) (Sahenk et al.;2005). Larger scale studies are lacking to confirm these findings.

Therapy with the progesterone receptor antagonist Onapristone, a regulator of Pmp22 and Mpz genes in cultured Schwann cells, reduced the PMP22 overexpression in a CMT1A rat model to a degree at which the axonal support function of Schwann cells is better maintained than myelination in later disease stage. Despite these promising results for the treatment of CMT1A, unacceptable toxicity was expected for humans (Sereda et al., 2003; Meyer zu Horste, 2007).

Another interesting agent that is currently under clinical investigation is ascorbic acid, which is necessary for peripheral nerve myelination both in vivo and in vitro. Chronic high dose application of ascorbic acid resulted in prolonged survival and clinical improvement in a CMT1A mouse model (Passage et al., 2004;). Nevertheless, clinical studies in humans showed no significant improvement in patients after one (Verhamme et al.,2009; Micallef et al., 2009; Burns et al., 2009) or two years (Pareyson et al., 2011) of treatment. Furthermore, important gastrointestinal adverse effects were seen in half of the patients with the highest dose (5 grams daily).

The curry spice derivate Curcumin was proposed as a causal working agent for those CMT types in which accumulation of cytotoxic proteins is involved in disease pathogenesis. It stimulates misfolded proteins to migrate from the endoplasmatic reticulum to the cell membrane, thereby removing cytotoxic components from the cytoplasma. In a TremblerJ mouse model for CMT1, Curcumin has been proven to reduce apoptosis, increase axonal size and thickness of myelin and improve motor performance (Khajavi et al, 2007). Side effects were not reported thus far, but clinical trials with CMT patients are not available to confirm these positive findings (Singh et al., 2007).

The search for substances that can improve function or survival of degenerating neurons or neuroglia is the subject of ongoing research both in the central and peripheral nervous system (PNS). An interesting protein in this perspective is granulocyte colony stimulating factor (G-CSF). Granulocyte colony stimulating factor (G-CSF or CSF 3) is a glycoprotein produced by monocytes, fibroblasts, endothelial and mesothelial cells in humans. It stimulates the proliferation, differentiation and specific cell function activation of neutrophil progenitor cells in the bone marrow (Roberts et al., 2005; Anderlini et al., 2008). Beside this main site of action, G-CSF has functional receptors (G-CSF-R) on other hematopoietic cell types like monocytes, platelets, activated T-cells and dendritic cells, and extra-hematopoietic cells including endothelium, placental, neurons and glial cells (Roberts et al., 2005). The mechanism of action of G-CSF in these cells is not completely understood, but seems to parallel the anti-apoptotic and proliferative effect on neutrophil progenitor cells. For more than two decades, recombinant human G-CSF has been used in clinical practice as a stimulator of white blood cell production in patients with neutropenia. It serves as an adjuvant treatment for leukemia and myelodysplasia. After the discovery of its capacity to mobilize stem cells from the bone marrow (Bussolino et al., 1987), it gained a place in the preparation of bone marrow from donor patients. It has been thoroughly tested and approved safe for humans, with serum hyperviscosity syndrome (due to granulocytosis) and bone pain as main adverse effects (Welte et al., 1996).

The discovery of G-CSF receptors (G-CSF-R) in the central nervous system (CNS) has been subject of multiple studies over the last ten years. The G-CSF-R is expressed by neurons in virtually all areas of the brain (Diederich et al., 2007). Growing evidence depicts a neuroprotective role for G-CSF by inhibition of programmed cell death and stimulation of neuronal progenitor proliferation and differentiation. In animal models for cerebral ischemia,

G-CSF attenuated the inflammatory cascade and potentiated angiogenesis (Schneider et al., 2005). Furthermore, G-CSF was shown to mobilize neural stem cells from the bone marrow, which suggests regenerative opportunities in the CNS (Shyu et al. 2004). In rodent models for stroke, diminished infarct size, improved functional recovery and survival were observed following G-CSF administration (Schabitz et al., 2003; Six et al., 2003; Gibson et al., 2005). These findings have led to clinical trials investigating G-CSF as a candidate therapy for stroke (for review see Bath et al., 2007 and England et al., 2009) and other neurodegenerative diseases including Parkinson's disease (Cao et al., 2006; McCollum et al., 2010), amyotrophic lateral sclerosis (Pitzer et al., 2008; Henriques et al., 2010; Chiò et al, 2011) and Alzheimer's disease (Tsai et al., 2007; Sanchez-Ramos, 2009; Zao et al., 2011).

The suggested functions of G-CSF in the CNS sparked the interest to investigate its effects in the PNS. To date, no studies have been published that investigated the presence of G-CSF receptors (G-CSFR) in the PNS or the role of G-CSF in peripheral nerve disease. Our hope is that the investigation of a potential function of G-CSF in the PNS may reveal findings similar to those in the CNS, so it can open a window for a regenerative therapy for hereditary neuropathies and perhaps other degenerative peripheral nerve diseases.

## Research goals

The aim of the research project was to investigate the effects of G-CSF in CMT disease, using a rat model of CMT1A. The obtained *in vivo* data may, in the best scenario, serve as a basis to evaluate G-CSF as a therapeutic agent for hereditary neuropathies in human clinical trials.

The research project ensued previous unpublished studies at our centre on the role of G-CSF in the PNS. In these preceding investigations, the expression of G-CSF and its receptor in primary rat Schwann cells (RSC), motoneurons, dorsal root ganglia neurons (DRGs) and sciatic nerves was studied *in vitro* and *in vivo* (Kleffner e.a., unpublished) . In addition to the expression pattern of G-CSF and its receptor in these cells, it was found that G-CSF exhibits proliferative and anti-apoptotic effects in primary rat Schwann cells, motoneurons and DRGs. It was clarified via which pathway G-CSF exerts these influences on the cell cycle in RSC and different pathways were explored with this purpose. Of special interest were the adenylat cyclase, MAPK/ERK, PI3K and JAK/STAT signal transduction pathways. It was studied how these effects correlated with myelination and myelin maintenance *in vitro*.

The findings above suggest a beneficial role for G-CSF in the survival, proliferation and function of Schwann cells that may enhance proper PNS myelination. It makes G-CSF an protein of interest with possible therapeutic potential for demyelinating hereditary neuropathies and perhaps acquired demyelinating neuropathies. To further investigate its therapeutic potential, we designed a pilot-study in which the histological, electrophysiological and vascular effects of G-CSF on peripheral nerves of a CMT animal model were investigated in a blinded, randomized, placebo-controlled fashion. We chose a CMT1A rat model that contains a duplication of the PMP22 gene, the PMP22<sup>+/+</sup> transgenic rat, because it has proven to be a reliable model that mimics well the clinical and histological features of human CMT1A patients and has early-onset pathology. In immature animals, we examined if the daily administration of G-CSF during two weeks from the third week after birth, could prevent or improve the histological and electrophysiological features of the PMP22<sup>+/+</sup> transgenic rat. The next step would be to administer the same treatment schemes in adolescent animals, to verify if G-CSF can ameliorate the disease course once neuropathological features have clearly developed. If the findings of the pilot-study support the role of G-CSF as a protective or regenerative agent in CMT1A, the conduct of a larger long-term animal trial would be planned that could pave the way to a clinical trial of G-CSF in CMT1A patients.

# Materials and methods

## Animal model

PMP22<sup>+++</sup> transgenic CMT1A Sprague Dawley rats were provided by M. Sereda and his team. Routine genotyping was performed by polymerase chain reaction (PCR), using genomic DNA from ear biopsies and mouse transgene-specific primers under standard conditions as described previously (Pareyson et al., 2009). The study animals were kept in standard housing conditions in mixed cages together with their mother, with a 12-hours light dark cycle and free access to food and water. The animals were daily evaluated clinically using a standardized clinical list for evaluating rodents as required by the ethical committee. All procedures and animal studies were performed in concordance with and approved by the local governmental authority Landesamt für Natur, Umwelt und Verbraucherschutz (Study approval number 8.87-51.04.20.09.347 on 17.08.2009) and the European Convention for Animal Care and Ethical Use of Laboratory Animals. The number of animals was kept to the minimum.

## Interventions

Ear biopsies for genetic analysis and animal identification were taken on postnatal day 14. PMP22<sup>+++</sup> transgenic CMT1A rats and wild-type rats were treated with G-CSF (case) or placebo (control) from postnatal day 15 until day 30. Different doses of subcutaneous G-CSF, 10/ 50/100 µg/kg per day or placebo (NaCl 0.9%), were applied once daily during 15 subsequent days. The treatment protocol was derived from stroke studies in murine models with short (<10 days) subcutaneous G-CSF administration dosed 10 to 100 µg/kg (Gibson et al., 2005; Sehara et al., 2007; Six et al., 2003; Solaroglu et al., 2006; 2009, 26,47,48 Shyu et al., 2004; Yanqing et al., 2006; Taguchi et al., 2007). G-CSF was provided as Filgrastim (Neupogen® - Amgen Inc) subcutaneous injection solution. Safety of repeated Filgrastim administration has previously been established in the rat in both subacute and chronic settings. Subcutaneous administration showed no significant toxicity with doses up to 3450 µg/kg in these studies (For pre-clinical experience see [http://www.accessdata.fda.gov/drugsatfda\\_docs/label/2002/filgamg052902PLBp1.pdf](http://www.accessdata.fda.gov/drugsatfda_docs/label/2002/filgamg052902PLBp1.pdf)). The animals were randomly assigned to treatment or placebo groups. Injections were given subcutaneous in the neck fat pads by the same investigator following weight measurement to

daily adjust the individual doses. The investigator was blinded for the genotype and treatment of the animals. Blood samples were taken from the tail vein on postnatal day 16 in at least four animals per treatment group. At this time, the rats had received two administrations of G-CSF. A time-frame of 18 hours after the second G-CSF injection preceded the blood collection.

### **Electrophysiological evaluation**

Electrophysiological analysis was performed on caudal nerves in living anesthetized animals, 24 hours after the last administration of G-CSF or placebo (postnatal day 31). Nerve conduction velocity (NCV) and compound muscle action potential (CMAP) of the caudal nerve were determined by tail recordings by the same examiner who was blinded for the genotype and treatment of the animals. The rats were anesthetized with a mixture of Ketamine (100 mg/kg) and Xylazine (20 mg/kg) and placed under an infrared warmth lamp to stabilize temperature before and after the procedure. During the EMG measurement, body temperature was maintained at 37°C by placing the rats on a heat pad, monitoring temperature with a rectal probe. CMAP recordings from tail muscles to single electric stimuli of 0.1 millisecond duration to the tail nerves were recorded via fine subcutaneous needle electrodes connected to a Toennies NeuroScreen system (Jaeger). NCV's were calculated automatically from the latency difference between the CMAP's after successive proximal stimulation at two sites 20 mm apart. CMAP amplitudes were calculated peak to zero line.

### **Tissue Preparation**

After 15 days of treatment (postnatal day 31), all rats were killed by isoflurane inhalation after the electrophysiology procedure. The animals were perfused with 0.9% NaCl solution for 5 minutes and, in case of Epon embedding, with 4% paraformaldehyde for 15 minutes. After perfusion, sciatic and tibial nerves were immediately dissected entirely from its spinal origin up to the medial ankle, and embedded in Epon epoxy or frozen in Tissue Tek according to previously published protocols (Serada et al. 2006, Carenini 2001). The liver, thymus and spleen were dissected entirely and weighted immediately.

## **Histological Evaluation**

Blood smears were investigated for cellular composition after Giemsa-staining with light microscopy, magnification 100x. White blood cell differentiation was performed by counting at least 200 white blood cells per animal, by an investigator who was blinded to the treatment groups. Morphological nerve studies of Epoxy epon embedded sections were performed with light microscopy on semithin sections (50µm) of the distal sciatic and tibial nerve (Ultracut 200 microtome, Leica). The sections were stained with alkaline toluidine blue 1% and photographed using a standard video frame grabber with 40x magnification (Leica) installed on a Zeiss Axiophot microscope (Zeiss). Overlapping photographs of the nerve were merged using Autostitch software (<http://www.cs.bath.ac.uk/brown/autostitch/autostitch.html>). The total number of axons (“total axon number”) per sciatic and tibial nerve was counted manually on cross sections by the same investigator in a blinded fashion using ImageJ cell counter (v1.36, National Institutes of Health). Physiologically unmyelinated axons (diameter <1µm) and blood vessels were not included. The nerve caliber (area) of sciatic and tibial nerve cross sections was calculated using ImageJ cell area calculator. The degree of demyelination and remyelination of axons was estimated visually in more than 1000 axons per animal. The area based myelin G-ratio, defined as the ratio between the inner and the outer diameter of the myelin sheath, was calculated to assess axonal myelination on cross sections in at least 200 axons per animal using ImageJ G-ratio Tool (CIF). For immunohistochemical analysis, semithin (10 µm) cross-sections of fresh frozen sciatic nerves were investigated with an Zeiss Axioplan2 immunofluorescence microscope connected to a Zeiss AxioCam MRc camera (AxioVision 3.1.). Blood vessel count was performed manually with ImageJ cellcounter on cross sections (minimum diameter > 1µm) . Blood vessels were visualized with rabbit-anti Von Willebrand Factor antibodies (Dakocytomation®) and secondary goat-anti-rabbit IgG AlexaFluor 594 (Invitrogen Molecular Probes®). Macrophages (circulation + tissue macrophages) were detected using mouse-anti ED2 (= CD163) primary antibodies (Serotec®) with goat-anti-mouse secondary IgG antibodies AlexaFluor 488 (Invitrogen Molecular Probes®). T-lymphocytes were detected using mouse-anti CD3 primary antibodies (BD Biosciences®) and goat-anti-mouse AlexaFluor 488 secondary antibodies. Granulocytes were stained with rabbit-anti-elastase (Abcam®) and goat-anti-rabbit AlexaFluor 488 secondary antibodies. Nuclei were stained with 4',6-diamidino-2-phenylindole (DAPI) for all analyses.

## **Statistical analysis**

Data was analyzed using SPSS statistic 19.0. Continuous variables were analyzed for normal distribution and compared with Student's t test for two groups and with the ANOVA tests for more than two groups, followed by post hoc analysis (LSD). A p-value of  $\leq 0.05$  double sided (Student's t test) or one sided (ANOVA), was considered significant. Results are reported as percentage for categorical variables, as mean  $\pm$  SD for normal distributed continuous values and as median with interquartile range (IQR) [25-75%] if not normal distributed. Outcome variables were nerve conduction velocity (m/s), compound muscle action potential (mV), nerve caliber (nerve area,  $\text{mm}^2$ ), total axon number and density (pro  $\text{mm}^2$ ), area based myelin G-ratio, demyelination percentage (%), inner and outer axon diameter ( $\mu\text{m}$ ), total blood vessel number and total blood vessel density (pro  $\text{mm}^2$ ), number of endoneural macrophages, granulocytes and lymphocytes.

# Results

## Subjects

A total of 50 animals, 33 PMP 22<sup>+/+</sup> case animals and 17 wild-type controls, were included. Animal distribution to dosing groups or placebo is displayed in table 1. One transgenic animal receiving 100 µg/kg G-CSF deceased on postnatal day 28. The animal displayed failure to thrive from the second week after birth, presumably due to the large litter size of 14 animals, rather than as a side effect of G-CSF.

During the 14 days of observation, there was no difference in general appearance, activity and behavior among transgenic and wild-type rats either treated with placebo or one of the three G-CSF doses. Average daily weight gain was comparable for all treatment groups and placebo (3.45 g/day for females and 3.06 g/day for males;  $p = 0.82$  resp.  $0.27$ ).

Animals treated with G-CSF showed a dose-dependent elevation of the relative and absolute number of neutrophils on differential blood counts (15.9% neutrophils (placebo), 17.0% (10 µg/kg G-CSF), 46.1% (50 µg/kg G-CSF) and 47.6% (100 µg/kg G-CSF);  $p = 0.001$ ; fig. 1A-B, table 2). They also displayed a dose dependent spleen enlargement (0.37% of total body weight (placebo), 0.41% (10 µg/kg G-CSF), 0.44% (50 µg/kg G-CSF), 0.49% (100 µg/kg G-CSF);  $p = 0.003$ ; table 2). Liver and thymus size was not significantly different between treatment and placebo groups.

**Table 1: Animal distribution to different G-CSF doses or placebo.**

	PMP 22 <sup>+/+</sup> (m:f) <sup>a</sup>	wild-type (m:f) <sup>a</sup>	total
placebo	8 (3:5)	5 (2:3)	13
10 µg/kg	7 (3:4)	3 (2:1)	10
50 µg/kg	9 (3:6)	4 (2:2)	13
100 µg/kg	9 (5:4) <sup>b</sup>	5 (3:2)	14
total	33	17	50

<sup>a</sup> m= male, f= female

<sup>b</sup> one transgenic male deceased on postnatal day 28

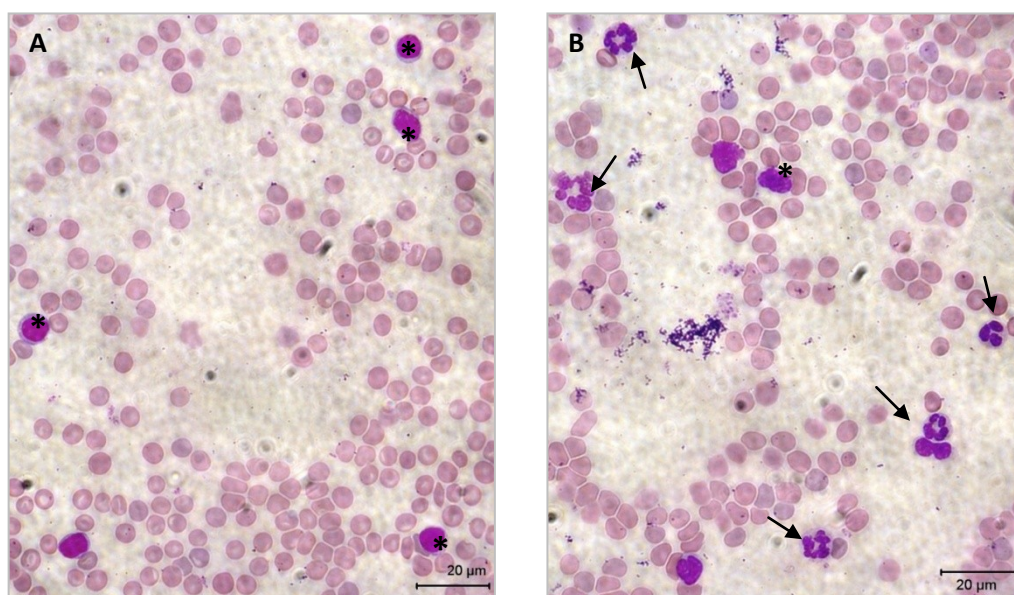


**Figure 1: Venous blood smears of wild-type rats receiving placebo (A) or G-CSF (B) (Giemsa staining, LM magnification 100x) . Smear A shows some lymphocytes (asterix) and no neutrophils. Smear B of a rat receiving 100 µg/kg G-CSF displays an elevated number of neutrophils (arrow) on treatment day 3.**

**Table 2: White blood cell differentiation and organometrics of rats aged resp. 3 and 4 weeks**

	placebo (n=5)	10 µg/kg G-CSF (n=4)	50 µg/kg G-CSF (n=4)	100 µg/kg G-CSF (n=5)	ref. values <sup>a</sup>
WBC differentiation					
lymphocyte (%)	80.7	80.25	51.9	50.4	83.2-87.7%
neutrophil (%)	15.9	17.0	46.1	47.6	7.0-13.3%
monocyte (%)	1.9.0	1.90	1.28	1.32	2.0-3.1%
basophil (%)	0.4	0.0	0.2	0.4	0.3-0.6%
eosinophil (%)	1.0	0.9	1.5	2.8	0.8-1.0%
organometrics					
liver (%TBW) <sup>b</sup>	4.7	4.3	4.6	4.5	not available
spleen (%TBW) <sup>b</sup>	0.37	0.41	0.44	0.49	not available
thymus (%TBW) <sup>b</sup>	0.51	0.53	0.57	0.56	not available

<sup>a</sup> Reference values source: Charles River laboratory hematology chart for male Sprague-Dawley rats aged 3-7 weeks

<sup>b</sup> TBW= total body weight

## Electrophysiology

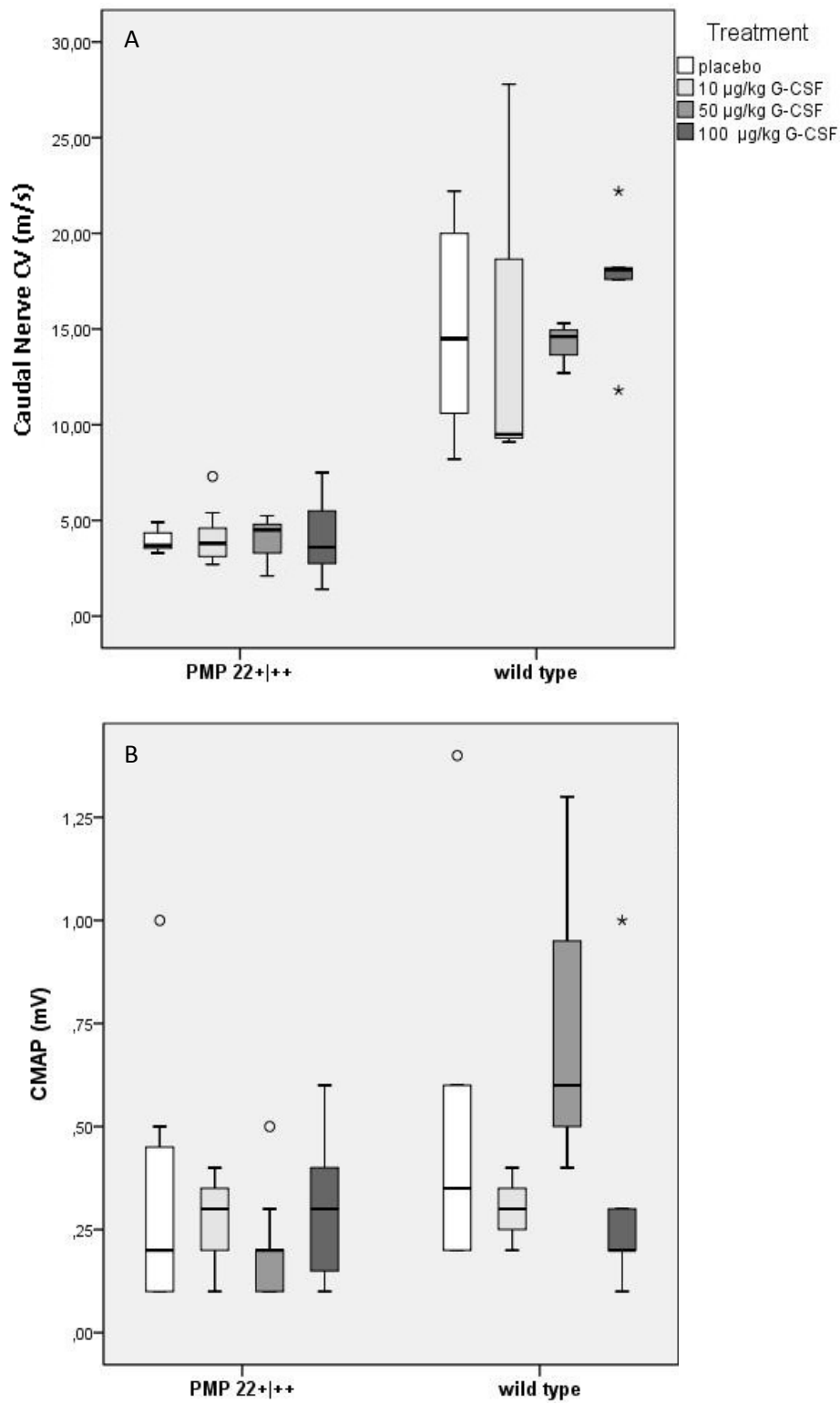
The caudal nerve conduction velocity (NCV) was measured in 49 animals, 17 wild-type and 32 PMP22<sup>+/+</sup> transgenic animals. We could not produce a consistent NCV measurement (no muscle action potential detectable) in one transgenic animal treated with 100 µg/kg G-CSF and one wild-type animal treated with 50 µg/kg G-CSF, which excluded them from analysis. Mean caudal NCV was more than three times lower in PMP22<sup>+/+</sup> transgenic rats compared to wild-types (4.1 ±1.39 m/s vs 15.7 ±5.44 m/s;  $p < 0.001$ ; fig. 2A). The compound muscle action potential (CMAP) amplitude at the distal stimulation site was significantly decreased in transgenic animals compared to wild-types (0.3 ± 0.20 mV vs 0.5 ± 0.40 mV;  $p = 0.02$ ; fig. 2B). We did not find a statistically significant difference in the caudal NCV or CMAP amplitude between transgenic animals receiving G-CSF treatment in any dosage and those receiving placebo ( $p = 0.957$  resp.  $0.788$ ; table 3; fig. 2A-B).

**Table 3: Mean caudal nerve conductance velocity (NCV) and compound muscle action potential (CMAP) for transgenic and wild-type rats treated with G-CSF compared to placebo.**

	mean NCV (m/s)	$p^a$	mean CMAP (mV)	$p^a$
<b><i>PMP 22<sup>+/+</sup></i></b>				
placebo (n=8)	3.9 ±0.56	0.957	0.23 ±0.16	0.788
10 µg/kg (n=7)	4.2 ±1.62		0.26 ±0.11	
50 µg/kg (n=9)	4.1 ±1.09		0.20 ±0.13	
100 µg/kg (n=7)	3.8 ±2.1		0.27 ±0.20	
<b><i>wild-type</i></b>				
placebo (n=5)	15.9 ±5.82	0.896	1.06 ±0.963	0.286
10 µg/kg (n=3)	15.5 ±10.68		0.30 ±0.100	
50 µg/kg (n=3)	14.2 ±1.34		0.77 ± 0.473	
100 µg/kg (n=5)	17.5 ±3.96		0.36 ±0.163	

<sup>a</sup> one-way ANOVA; significance level  $p < 0.05$

**Figure 2A-B: Box-and-whiskerplots of (A) caudal nerve conduction velocity (NCV) and (B) compound muscle action potential (CMAP) in PMP22<sup>+/+</sup> transgenic rats and wild-types. Outliers are marked by °, IQR with small group size is marked by \***



## Nerve Histology

### *Sciatic nerve histology*

Morphological analysis of distal sciatic nerve cross sections embedded in Epon epoxy was performed in 33 rats: 22 PMP22<sup>+/+</sup> transgenic rats and 11 wild-types (table 4, fig. 3). The total axon number and axon density were comparable for wild-types and PMP22<sup>+/+</sup> transgenic animals (table 4, fig. 4A). The sciatic nerve caliber (“sciatic nerve area”) was increased with 10% in PMP22<sup>+/+</sup> transgenic rats compared to wild-types ( $p= 0.038$ ; table 4, fig. 4B). The number of demyelinated axons and the area based G-ratio were significantly increased in PMP22<sup>+/+</sup> transgenic animals compared to wild-types, confirming the presence of demyelination in transgenic animals at the age of 4-weeks (table 4, fig. 4C-D).

Among the PMP22<sup>+/+</sup> transgenic animals, there was no statistically significant difference in the mean total axon number and density or in the extend of demyelination of the sciatic nerve in animals receiving G-CSF or placebo (table 5 and 6, fig. 4A-D).

**Table 4: Total axon number, axon density, nerve area, demyelination and G-ratio in sciatic nerves of wild-type and PMP22<sup>+/+</sup> rats.**

	wild-type (n=11)	PMP22 <sup>+/+</sup> (n=22)	$p^a$
total axon number	4514 $\pm$ 485.4	4503 $\pm$ 623.8	0.958
axon density ( $\times 10^2/\text{mm}^2$ )	53.5 $\pm$ 5.35	49.0 $\pm$ 7.47	0.590
nerve area ( $\text{mm}^2$ )	0.85 $\pm$ 0.06	0.93 $\pm$ 0.01	0.038*
demyelination (%)	3.5 $\pm$ 2.69	10.4 $\pm$ 3.10	0.001*
inner axon diameter ( $\mu\text{m}$ )	8.4 $\pm$ 0.99	6.4 $\pm$ 0.55	<0.001*
outer axon diameter ( $\mu\text{m}$ )	14.1 $\pm$ 1.14	10.7 $\pm$ 0.58	<0.001*
area based G-ratio	0.55 $\pm$ 0.028	0.60 $\pm$ 0.040	0.001*

<sup>a</sup> Student’s t test; significance level  $p < 0.05$  (\*)

**Table 5: Axon number, nerve area, axon density and demyelination in sciatic nerves of transgenic and wild-type rats receiving G-CSF or placebo.**

	total axon number	<i>p</i> <sup>a</sup>	nerve area (mm <sup>2</sup> )	<i>p</i> <sup>a</sup>	axon density (x10 <sup>2</sup> /mm <sup>2</sup> )	<i>p</i> <sup>a</sup>	demyelination (%)	<i>p</i> <sup>a</sup>
<b><i>PMP 22</i><sup>+/+</sup></b>								
placebo (n=5)	4467 ±399.0	0.890	0.92 ±0.075	0.538	48.9 ± 6.80	0.268	11.0 ±4.37	0.757
10 µg/kg (n=6)	4568 ±816.9		0.90 ±0.082		50.6 ±6.96		10.2 ±2.16	
50 µg/kg (n=6)	4616 ±562.9		0.90 ±0.191		52.2 ±6.52		9.4 ±2.93	
100 µg/kg (n=5)	4320 ±726.1		1.00 ±0.077		43.5 ±8.63		11.4 ±3.73	
<b><i>wild-type</i></b>								
placebo (n=3)	4665 ±631.7	0.753	0.84 ± 0.069	0.940	55.5 ±7.87	0.820	4.1 ±3.50	0.713
10 µg/kg (n=2)	4681 ±226.2		0.87 ±0.023		53.6 ±3.99		1.8 ±0.50	
50 µg/kg (n=3)	4448 ±654.8		0.84 ±0.094		52.7 ±2.92		4.5 ±3.90	
100 µg/kg (n=3)	4267 ±267.3		0.83 ±0.069		51.4 ±5.50		2.8 ±0.36	

<sup>a</sup>ANOVA; significance level p <0.05 (\*)

**Table 6: Area based G-ratio, inner and outer axon diameter in sciatic nerve sections for transgenic and wild-type rats receiving G-CSF or placebo.**

	G-ratio	$p^a$	inner perimeter ( $\mu\text{m}$ )	$p^a$	outer perimeter ( $\mu\text{m}$ )	$p^a$
<b><i>PMP 22<sup>+/+</sup></i></b>						
placebo (n=5)	0.61 $\pm$ 0.027	0.158	6.93 $\pm$ 0.611	0.047*	11.21 $\pm$ 0.630	0.139
10 $\mu\text{g}/\text{kg}$ (n=6)	0.60 $\pm$ 0.033		6.52 $\pm$ 0.515		10.80 $\pm$ 0.462	
50 $\mu\text{g}/\text{kg}$ (n=6)	0.58 $\pm$ 0.018		6.03 $\pm$ 0.402		10.35 $\pm$ 0.459	
100 $\mu\text{g}/\text{kg}$ (n=5)	0.57 $\pm$ 0.029		6.19 $\pm$ 0.388		10.74 $\pm$ 0.632	
<b><i>wild-type</i></b>						
placebo (n=3)	0.58 $\pm$ 0.013	0.334	8.55 $\pm$ 1.451	0.746	14.17 $\pm$ 2.300	0.743
10 $\mu\text{g}/\text{kg}$ (n=2)	0.54 $\pm$ 0.051		8.39 $\pm$ 1.085		14.34 $\pm$ 0.442	
50 $\mu\text{g}/\text{kg}$ (n=3)	0.55 $\pm$ 0.028		8.67 $\pm$ 0.765		14.71 $\pm$ 0.983	
100 $\mu\text{g}/\text{kg}$ (n=3)	0.55 $\pm$ 0.018		7.78 $\pm$ 0.554		13.32 $\pm$ 0.875	

<sup>a</sup>ANOVA; significance level  $p < 0.05$  (\*)

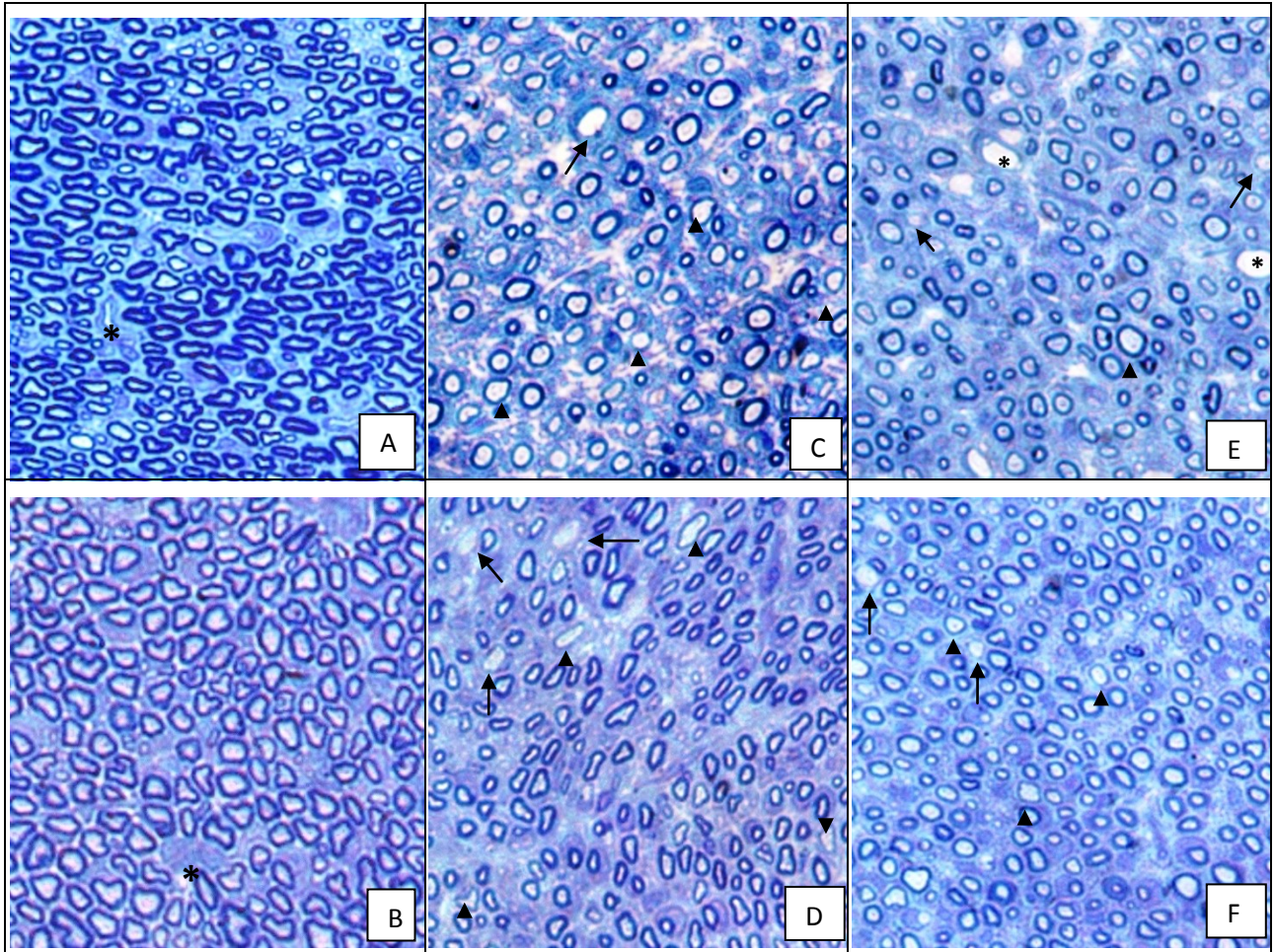


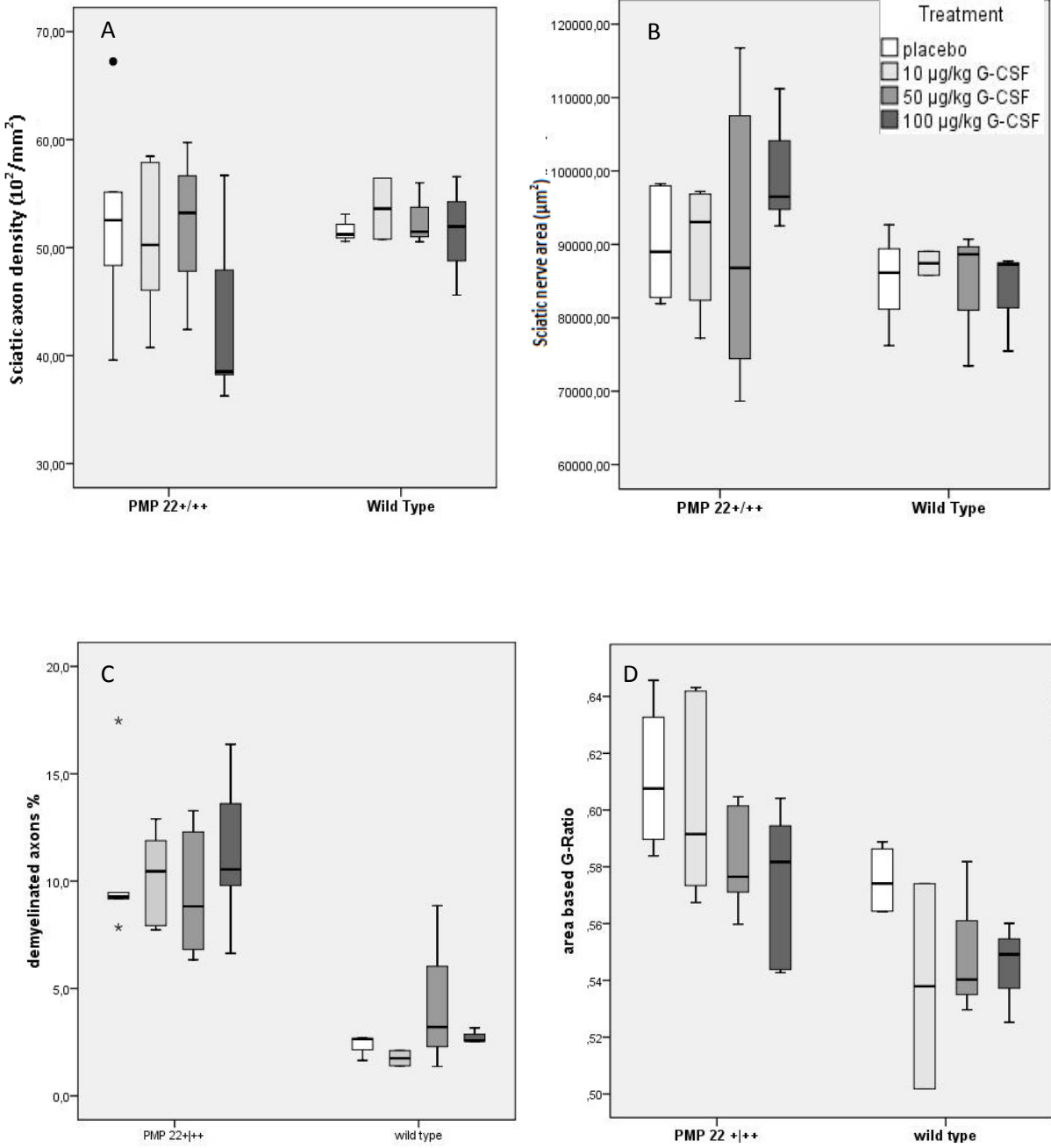
**Figure 3: Peripheral nervous system hypomyelination in PMP22<sup>+++</sup> transgenic rats (LM, magnification 40x).**

A-B: Semithin (50 μm) transverse sections of sciatic (A) and tibial (B) nerves from a wild-type rat showing normal myelin sheet thickness relative to axon size. Small blood vessels are also visible (asterix).

C-D: Semithin (50 μm) transverse sections of sciatic (C) and tibial (D) nerve from a PMP22<sup>+++</sup> transgenic rat receiving placebo. Hypo-myelinated (arrowhead) and a-myelinated axons (arrow) are surrounded by normal myelinated axons.

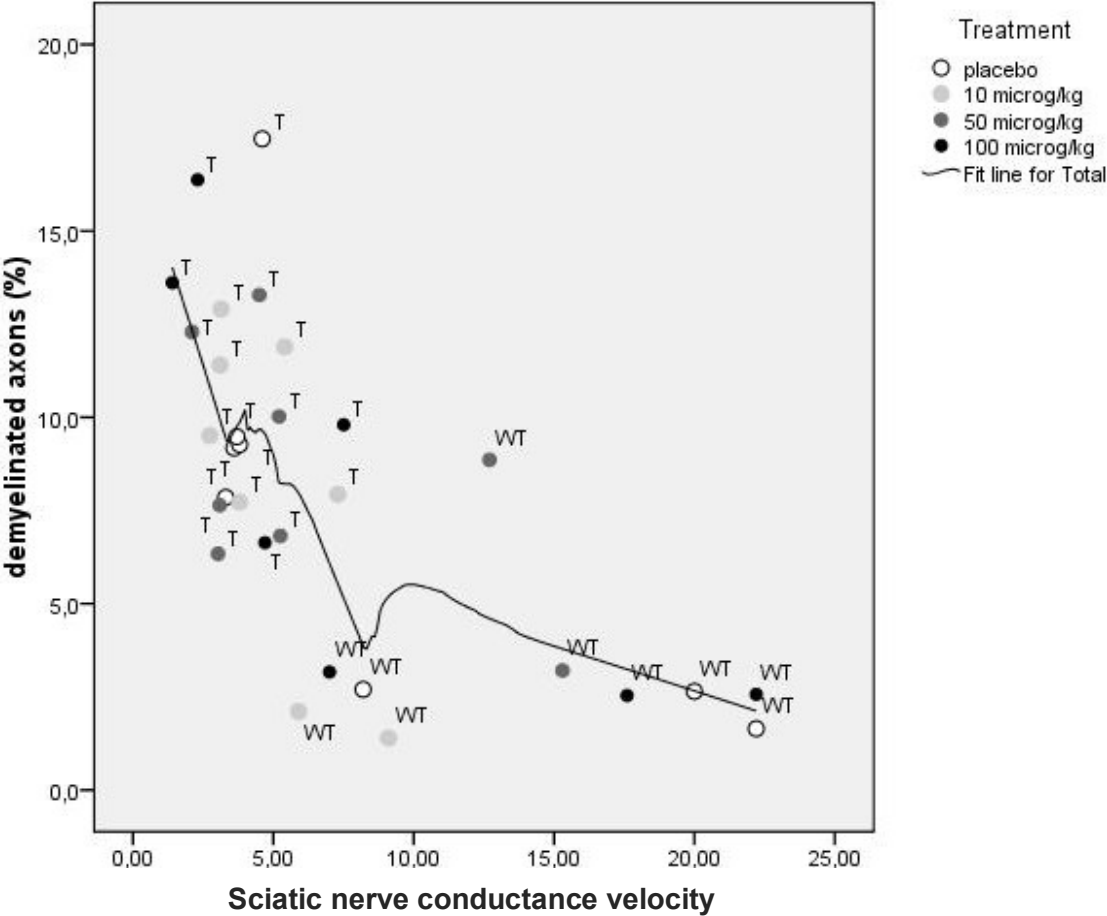
E-F: Semithin (50 μm) transverse sections of sciatic (E) and tibial (F) nerve from PMP22<sup>+++</sup> transgenic animals receiving 100 μg/kg G-CSF . Hypo-myelinated (arrowhead) and a-myelinated axons (arrow) are present among normal myelinated axons.

**Figure 4 A-D: Box-and-whiskerplots of sciatic axon density (A), nerve area (B), demyelination % (C) and area based G-Ratio (D) for transgenic and wild-type rats receiving G-CSF or placebo. Outliers are marked by●, IQR with small group size is marked by \***



Comparing the histological findings in sciatic nerves with the electrophysiological data of the caudal nerve, a strong correlation is observed between the extend of demyelination and the NCV: demyelination correlated with slower sciatic NCVs (Pearson's rho = - 0.659; p<0.001 (2-tailed), fig. 5).

Figure 5: Scatterplot sciatic nerve conduction velocity and demyelination, Pearsons Rho = -0.66.



## ***Tibial nerve histology***

Because CMT1A is a length-dependent neuropathy, we studied the effects of G-CSF on the morphology of the distally located tibial nerve. Histological analysis was performed on distal tibial nerve biopsies of 23 animals, 20 PMP22<sup>+/+</sup> transgenic and 3 wild-type animals (table 7, fig. 3 B, D, F).

The total axon density of the tibial nerve was reduced in PMP22<sup>+/+</sup> transgenic animals compared to wild-types (table 7, fig. 6A). The tibial nerve caliber (“nerve area”) was not significantly different between PMP22<sup>+/+</sup> transgenic and wild-type animals (table 7). The percentage of demyelinated axons was seven times higher in PMP22<sup>+/+</sup> transgenic animals compared to wild-types (table 7, fig. 6B).

We did not find statistically significant differences in the extend of demyelination or axonal loss in the distal tibial nerve between transgenic animals receiving treatment or placebo (Table 8 and 9; fig. 7A-B).

**Table 7: Axon count, demyelination, area and G-ratio in tibial nerves**

	Wild-type (n=3)	PMP22 <sup>+/+</sup> (n=20)	<i>p</i> <sup>a</sup>
total axon number	2628 ±66.4	2302±563.4	0.337
axon density ( x10 <sup>2</sup> /mm <sup>2</sup> )	59.6 ±3.67	51.5±6.05	0.037*
nerve area (mm <sup>2</sup> )	0.44 ±0.021	0.45 ±0.098	0.938
demyelination (%)	1.1 ±0.74	7.0 ±2.90	0.024*
inner axon diameter (µm)	7.10 ±0.916	5.51 ±0.440	0.001*
outer diameter (µm)	13.21 ±1.181	9.92 ±0.617	0.001*
area based G-ratio	0.53 ±0.015	0.54 ±0.017	0.3475

<sup>a</sup>Student’s t test; significance level *p* <0.05 (\*)

**Table 8: Total axon count, nerve area, axon density and demyelination in tibial nerve sections from transgenic and wild-type rats receiving G-CSF or placebo.**

	total axon count	$p^a$	nerve area (mm <sup>2</sup> )	$p^a$	axon density (x10 <sup>2</sup> /mm <sup>2</sup> )	$p^a$	demyelination (%)	$p^a$
<b><i>PMP 22</i><sup>+/+</sup></b>								
placebo (n=5)	2418 ±518.0	0.883	0.50 ±0.088	0.549	48.7 ±5.91	0.553	6.8 ±2.85	0.198
10 µg/kg (n=5)	2269 ±716.4		0.43 ±0.104		52.3 ±6.90		9.2 ±3.09	
50 µg/kg (n=5)	2120 ±624.7		0.40 ±0.111		52.9 ±5.65		5.2 ±2.42	
100 µg/kg (n=5)	2375 ±571.1		0.49 ±0.158		48.9 ±3.62		6.7 ±2.85	
<b><i>Wild-type (n=3)</i></b>	2628 ±66.4		0.44 ±0.021		59.6 ±3.67		1.1 ±0.74	

<sup>a</sup>One-way NOVA; significance level  $p < 0.05$  (\*)

**Table 9: Area based G-ratio, inner axon and outer nerve perimeter in tibial nerve sections from transgenic and wild-type rats receiving G-CSF or placebo.**

	G-ratio	$p^a$	inner perimeter (µm)	$p^a$	outer perimeter (µm)	$p^a$
<b><i>PMP 22</i><sup>+/+</sup></b>						
placebo (n=5)	0.56 ±0.005	0.360	5.81 ±0.504	0.224	10.162 ±0.619	0.210
10 µg/kg (n=5)	0.54 ±0.019		5.20 ±0.358		9.434 ±0.477	
50 µg/kg (n=5)	0.53 ±0.012		5.46 ±0.302		9.927 ±0.608	
100 µg/kg (n=5)	0.53 ±0.030		5.56 ±0.591		10.157 ±0.762	
<b><i>Wild-types (n=3)</i></b>	0.53 ±0.015		7.10 ±0.916		13.21 ±1.181	

<sup>a</sup>One-way NOVA; significance level  $p < 0.05$  (\*)

**Figure 6 A-B: Box-and-whiskerplots of axon density (A) and degree of demyelination (B) of tibial nerve sections of PMP22<sup>+/+</sup> transgenic and wild-type animals receiving G-CSF or placebo.**

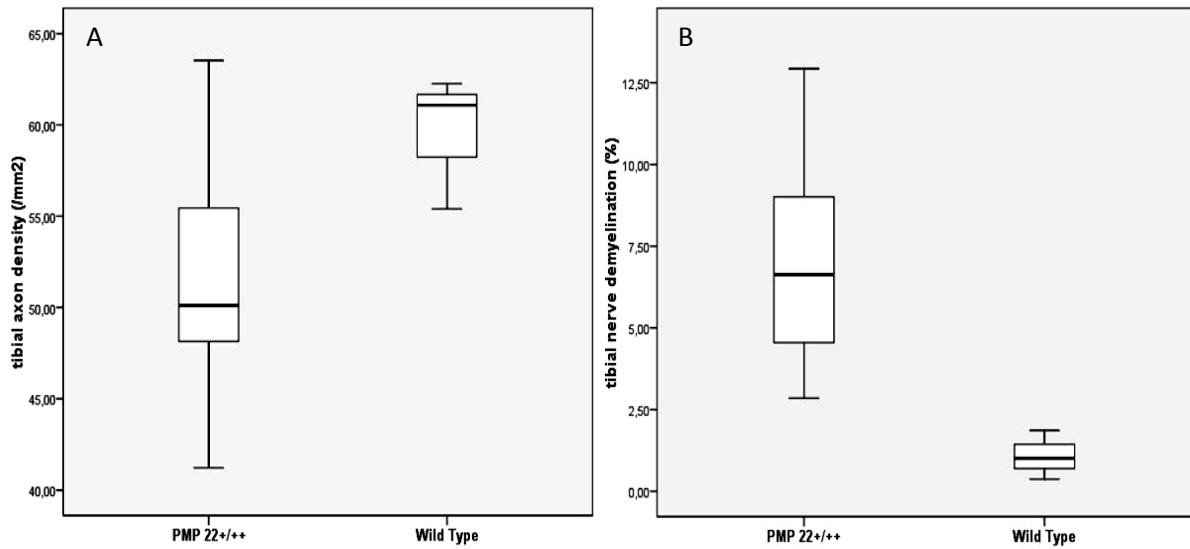
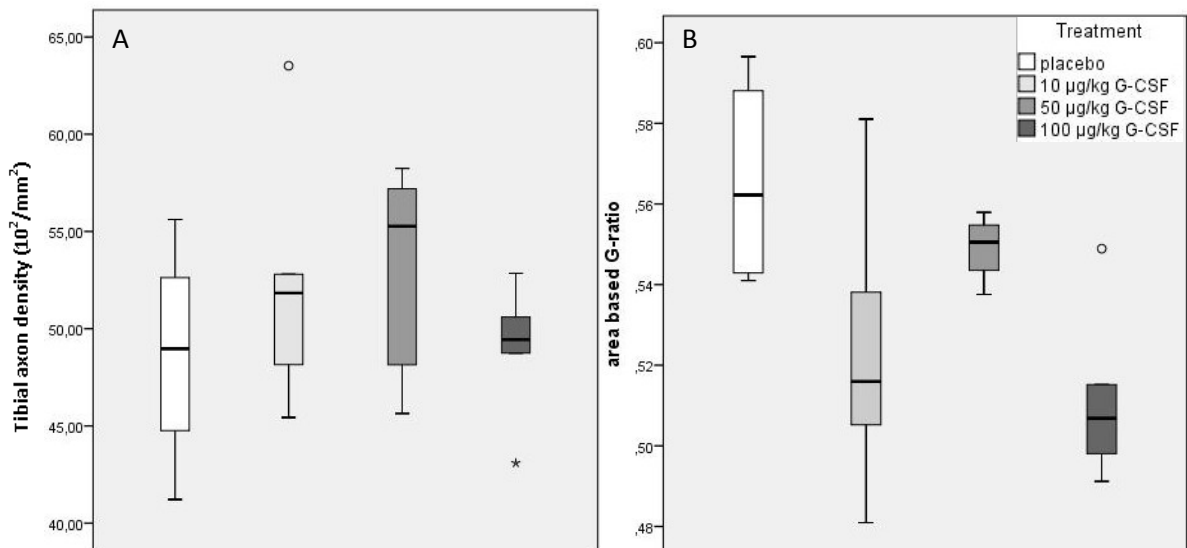


**Fig. 7 A-B: Box-and-whisker plots of tibial axon density (A) and G-ratio (B) for PMP 22<sup>+/+</sup> transgenic rats receiving G-CSF or placebo. Outliers are marked by °, IQR with small group size is marked by \***



## Nerve vascularization following G-CSF

Because G-CSF has been shown to induce angiogenesis and arteriogenesis in the CNS, it seemed interesting to study the effects of G-CSF on vascularization in the sciatic nerve of PMP 22<sup>+/+</sup> transgenic and wild-type rats. In order to obtain a first impression of nerve vascularization, we counted blood vessels on toluidine blue stained epoxy sections. We controlled and made our observations more precise using nerve immunohistochemistry for the Von-Willebrand factor, a component of endothelium.

### Toluidine blue stained blood vessel count

Blood vessels were counted manually on toluidine blue stained epoxy cross sections of the distal sciatic nerve from 33 animals, 22 PMP 22<sup>+/+</sup> transgenic and 11 wild-type animals. We observed a higher number of blood vessels per nerve section in transgenic animals compared to wild-types ( $48.6 \pm 27.31$  vs  $29.8 \pm 8.74 \times 10^2/\text{mm}^2$ ;  $p = 0.034$ , fig. 8A). This difference sustained with respect to the nerve area (“blood vessel density”,  $51.8 \pm 2.61$  per  $\text{mm}^2$  vs  $0.35 \pm 1.30$  per  $\text{mm}^2$ ;  $p = 0.054$ ; fig. 8B). We already reported that nerve caliber was larger in PMP 22<sup>+/+</sup> transgenic animals compared to wild-types ( $0.85 \pm 0.066 \text{ mm}^2$  vs  $0.92 \pm 0.120 \text{ mm}^2$ ;  $p = 0.029$ ).

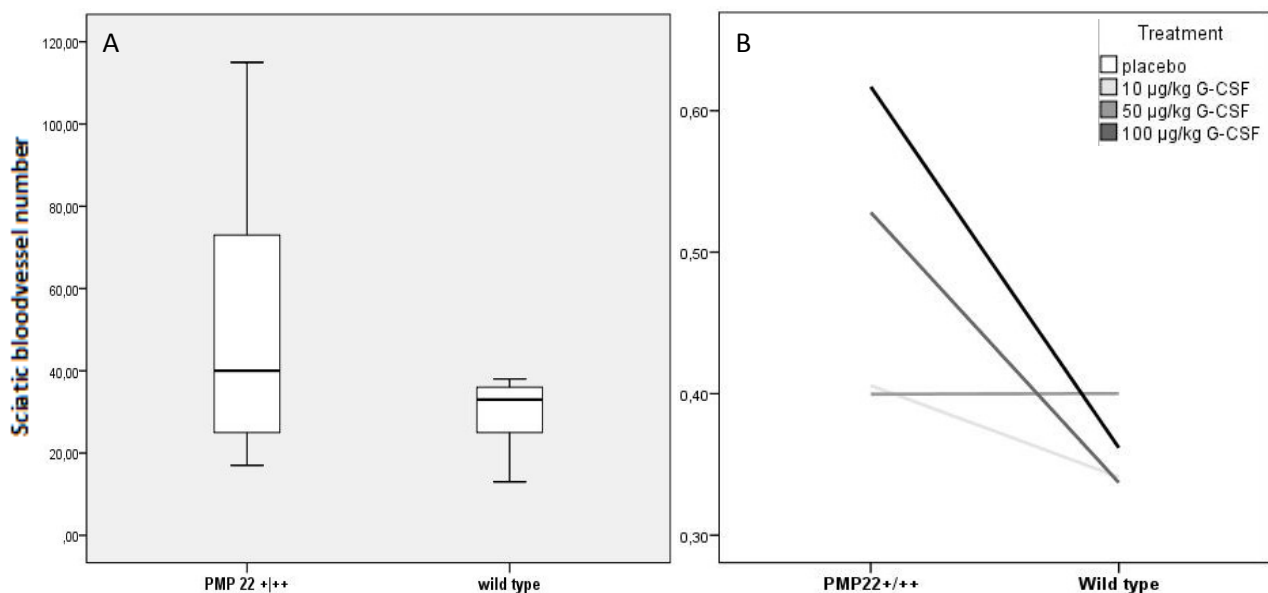


Figure 8: A: Box-and-whisker plots of bloodvessel count on toluidine blue stained sciatic nerve sections from transgenic and wild-type rats receiving G-CSF or placebo. B: Trend line of means of blood vessel density ( $\times 10^2/\text{mm}^2$ ) by G-CSF treatment or placebo.

Comparison of vascularization between animals treated with G-CSF and placebo, using this technique, revealed no significant dose-effect relation of G-CSF on vascularization (“blood vessel number”;  $p = 0.643$ , fig. 9A; ‘blood vessel density’  $p = 0.692$ , fig.9B).

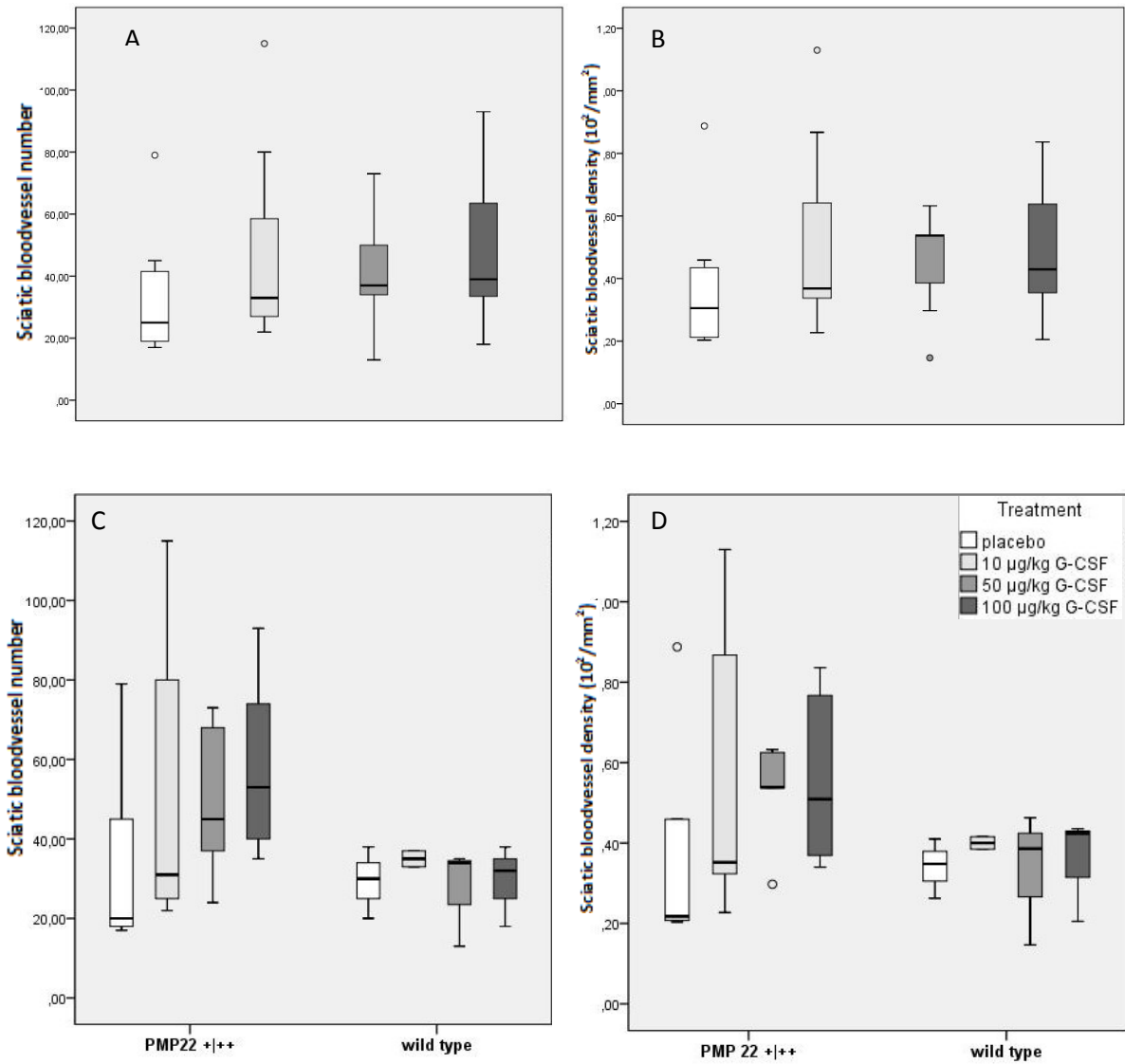
Within-group subanalysis of G-CSF or placebo treated PMP22<sup>+++</sup> transgenic and wild-type animals, showed no significant difference in blood vessel number or density between placebo and any of different concentrations of G-CSF (table 10, fig. 9C-D).

**Table 10: Blood vessel count, nerve area and blood vessel density on toluidine blue stained epoxy cross sections of sciatic nerves from PMP22<sup>+++</sup> transgenic and wild-type animals treated with G-CSF or placebo.**

	blood vessel count	$p^a$	blood vessel density (/ mm <sup>2</sup> )	$p^a$	nerve area (mm <sup>2</sup> )	$p^a$
<b><i>PMP 22<sup>+++</sup></i></b>						
placebo (n=5)	35.8 ±26.79	0.634	39.5 ±29.59	0.651	0.90 ±0.079	0.490
10 µg/kg (n=6)	50.7 ±38.11		54.2 ±36.63		0.90 ±0.082	
50 µg/kg (n=6)	48.7 ±18.91		53.8 ±12.15		0.90 ±0.019	
100 µg/kg (n=5)	59.0 ±24.26		62.0 ±21.93		1.00 ±0.077	
<b><i>Wild-type</i></b>						
placebo (n=3)	29.3 ±9.02	0.860	34.0 ±7.41	0.928	0.85 ±0.090	0.951
10 µg/kg (n=2)	35.00 ±2.83		40.0 ±2.19		0.87 ±0.023	
50 µg/kg (n=3)	27.3 ±12.42		33.2 ± 6.49		0.84 ±0.094	
100 µg/kg (n=3)	29.3 ±10.26		35.5 ±12.97		0.83 ±0.695	

<sup>a</sup> One-way NOVA; significance level  $p < 0.05$  (\*)

**Figure 9: Box-and-whisker plots of blood vessel number and density in toluidine blue stained sciatic nerve sections of PMP22<sup>+/+</sup> transgenic and wild type animals receiving G-CSF or placebo. A-B: grouped means. C-D: subgroup analysis in PMP22<sup>+/+</sup> transgenic and wild type animals. Outliers are marked by °.**



## Immunohistochemical study of vascularization

To enhance the accuracy of the observations above, we visualized endothelial cells in distal sciatic nerve sections by immunofluorescence microscopy using antibodies against the endothelial von Willebrand factor (anti-VWF) (fig. 10 A-B). A total of 16 animals were analyzed, 10 transgenic and 6 wild-type animals, randomly distributed to placebo, 50  $\mu\text{g}$  and 100  $\mu\text{g}$  G-CSF treatment. With this technique, we did not observe a significant difference in the number or density of blood vessels located in distal sciatic nerve sections of PMP22<sup>+/+</sup> transgenic animals compared to wild-types ( $27.2 \pm 5.16$  vs  $29.7 \pm 2.80$ ,  $p = 0.1789$ , fig. 11A-B).

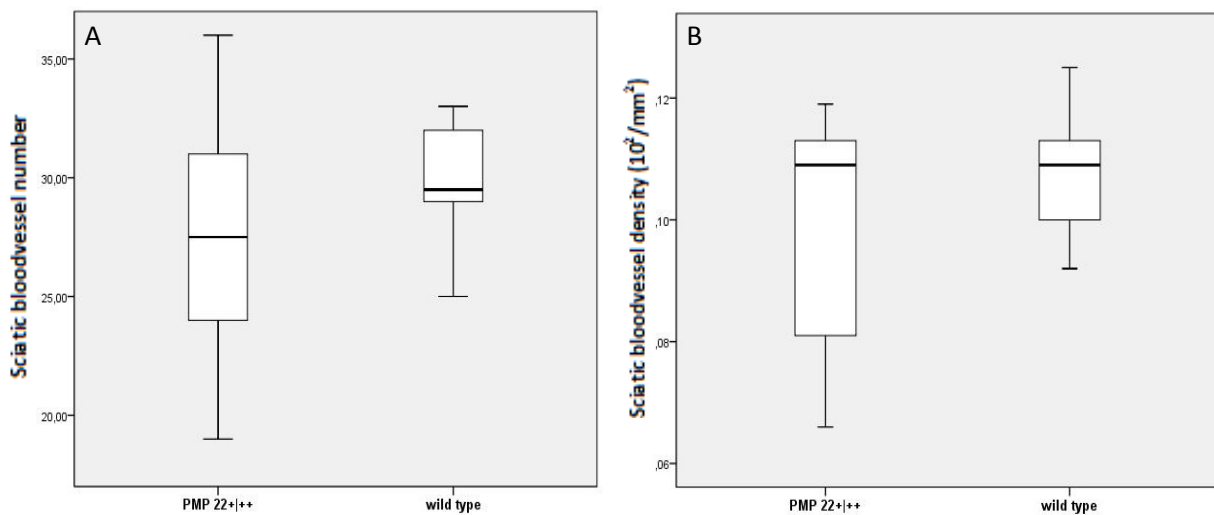
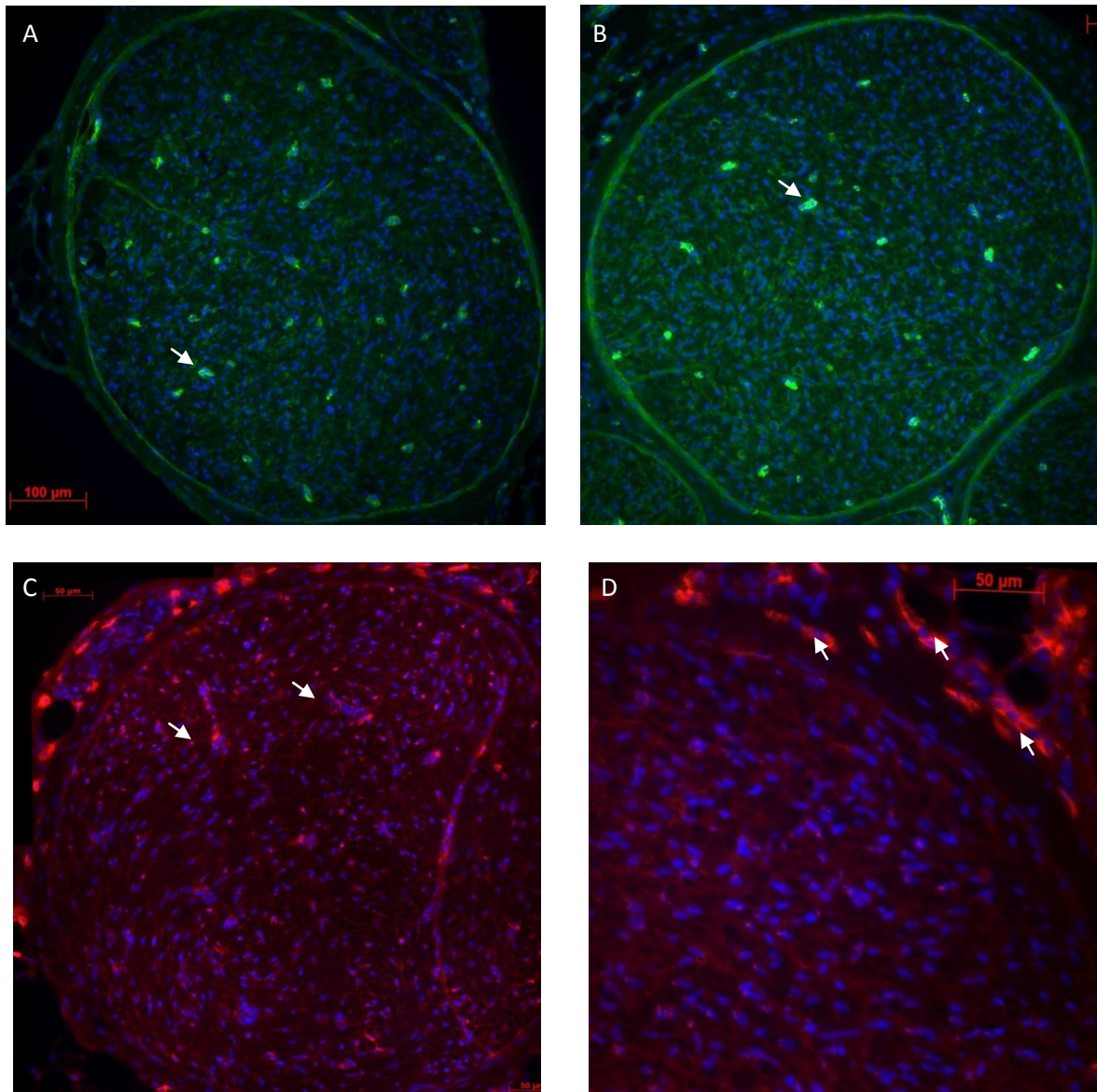


**Figure 11: Box-and-whisker plots of blood vessel number (A) and blood vessel density (B) on anti-VWF stained sciatic nerve sections from PMP 22<sup>+/+</sup> transgenic and wild-type rats receiving G-CSF or placebo.**

Comparing vascularization between the 50 and 100  $\mu\text{g}$  G-CSF treated animals and placebo, revealed a significant group-difference in vascularization ( $p = 0.048$ , Table 8, fig. 12A).

Between group and post-hoc analysis did not reveal a linear dose-effect response; but revealed the 50  $\mu\text{g}$  G-CSF dosing group to be lower in particular to the 100  $\mu\text{g}$  G-CSF dosing group (LSD post hoc,  $p = 0.015$ ) as well as to the placebo group.

**Figure 10 A-D: blood vessels and macrophages in sciatic nerves of PMP 22<sup>+/+</sup> transgenic rats**



A-B: Transverse cryosections of distal sciatic nerves from PMP22<sup>+/+</sup> rats receiving 100 µg/kg G-CSF (A) or placebo (B) were stained with anti-VWF to visualize blood vessels (green, arrows). Cell nuclei were stained with DAPI (blue). (IHC, 40x magnification)

C-D: Semithin transverse sections of frozen distal sciatic nerve from PMP22<sup>+/+</sup> rats receiving 50, 100 µg/kg G-CSF or placebo were stained with anti-ED2 to visualize endoneurial (C) and epineurial (D) macrophages (red, arrows). Cell nuclei were stained with DAPI (blue). (IHC, 40x magnification)

**Figure 12 : total blood vessel number and blood vessel density in sciatic nerves of PMP 22<sup>+/+</sup> transgenic and wild-type rats receiving placebo or 50 or 100 µg G-CSF (° outlier). A: grouped mean of blood vessel number. B-C: subgroup analysis in PMP 22<sup>+/+</sup> transgenic and wild-type rats.**

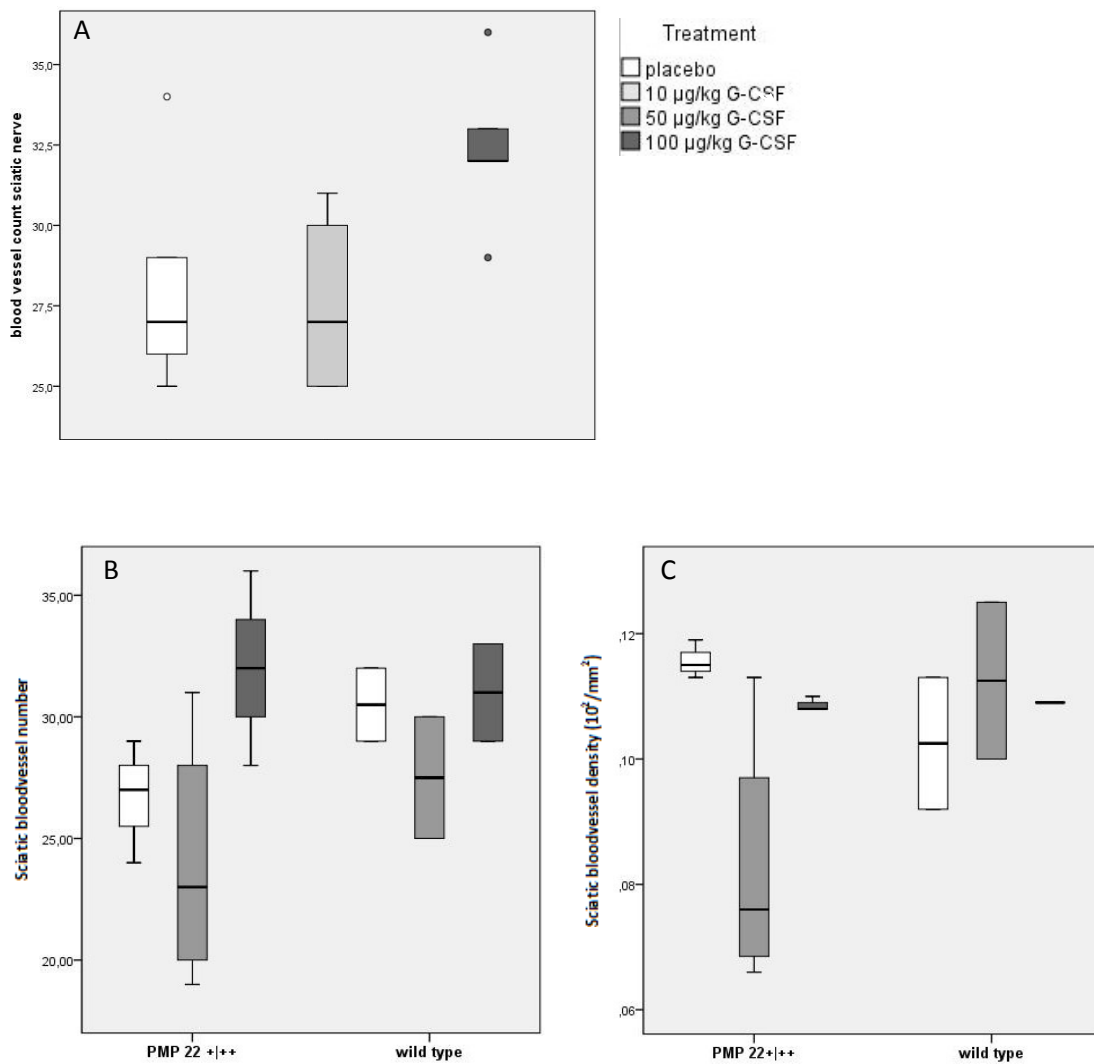


**Table 8: blood vessel count and blood vessel density in sciatic nerve**

	Blood vessel number	<i>p</i> <sup>a</sup>	Blood vessel density (pro mm <sup>2</sup> )	<i>p</i> <sup>a</sup>
Placebo (n=5)	28.2 ±2.94	0.048	11.0 ±1.07	0.164
50 µg/kg (n=6)	25.2 ±4.75		9.3 ±2.40	
100 µg/kg (n=5)	31.6 ±3.21		10.9 ±0.8986	

<sup>a</sup>One-way ANOVA test; significance level *p* <0.05 (\*)

Subanalysis among the two G-CSF dosing schemes and placebo for transgenic and wild-type animals suggested a significant group-difference in blood vessel density in PMP22<sup>+/++</sup> transgenic animals (Table 11, Fig. 12 B-C). Post-hoc analysis again did not reveal a linear dose-effect response, and also pointed out the 50 µg G-CSF dosing group to be lower with respect to the 100 µg G-CSF dosing group as well as to the placebo group. In other words, there was no significant raise of blood vessel density with increasing concentrations of G-CSF.

**Table 11: Blood vessel count and density (immunofluorescent method), nerve area for transgenic and wild-type rats; G-CSF compared to placebo**

	Blood vessel count	$p^a$	Blood vessel density (/ mm <sup>2</sup> )	$p^a$	Nerve area (mm <sup>2</sup> )	$p^a$
<b><i>PMP 22<sup>+/++</sup></i></b>						
placebo (n=3)	26.7 ±2.52	0.113	11.6 ±0.00	0.036	2.31 ±0.168	0.200
50 µg/kg (n=4)	24.0 ±5.29		8.3 ±0.21		2.92 ±0.149	
100 µg/kg (n=3)	32.0 ±4.00		11.1 ±0.00		2.95 ±0.295	
<b><i>Wild-type</i></b>						
placebo (n=2)	30.5 ±2.12	0.507	10.3 ±0.02	0.767	3.00 ±0.242	0.161
50 µg/kg (n=2)	27.5 ±3.54		22.3 ±0.02		2.45 ±0.068	
100 µg/kg (n=2)	31.0 ±2.80		9.0 ±0.00		2.84 ±0.269	

<sup>a</sup> One- way ANOVA test; significance level  $p < 0.05$

### ***The immune system: role in early CMT?***

Because macrophages and T-helper-2 lymphocytes are thought to play a local role in the pathophysiology of CMT, we investigated the presence of inflammatory cells in sciatic nerve sections. We also investigated if there were endoneural granulocytes present in the sections as a possible effect of the administration of G-CSF. Distal sciatic nerve sections of 16 animals were studied, 10 PMP 22<sup>+/+</sup> transgenic and 6 wild-type animals randomly distributed to three different dose groups (placebo, 50 µg and 100 µg G-CSF).

The sections were analyzed with immunohistochemical staining against CD163 (ED2) for the presence of tissue macrophages (fig. 10 C-D). We noticed a perineural clustering of tissue macrophages in the nerve sections with fewer endoneural macrophages. There was no significant difference in the number of endoneural macrophages in transgenic animals compared to wild-type controls ( $23.2 \pm 12.72$  in transgenic and  $32.5 \pm 11.02$  in wild-type animals, Student's t test,  $p = 0.170$ ). We did not find statistically significant differences in the number of endoneural macrophages between animals receiving placebo, 50 or 100 µg G-CSF treatment (resp.  $20.8 \pm 8.20$ ;  $24.8 \pm 9.30$  and  $34.8 \pm 17.05$ , One-Way ANOVA,  $p = 0.20$ ).

We could not visualize T-lymphocytes or granulocytes in the endoneurium with immunohistochemistry using antibodies to respectively CD3 and anti-elastase on subsequent sciatic nerve sections (not shown).

## Discussion

The main goal of this study was to examine the short-term effects of G-CSF on peripheral nerve myelination and axonal preservation in a rat model of CMT1A, the PMP22<sup>+/+</sup> rat. Additionally, we studied the effects of G-CSF on the vascularization and cellular immune response in peripheral nerves of PMP22<sup>+/+</sup> transgenic rats and wild-type animals.

Previous investigations conducted at our institute found evidence that G-CSF had proliferative and anti-apoptotic effects on primary cultured rat Schwann cells, motoneurons and dorsal root ganglion neurons in vitro (Kleffner et al. 2011, unpublished results). However promising, our study could not confirm these findings in a rat model of CMT1A at the electrophysiological or histological level after two weeks of subcutaneous G-CSF therapy.

### No place for G-CSF in the treatment of CMT?

Before concluding that there is no potential for G-CSF in the treatment of CMT(1A), it is important to consider the possibility of a false negative finding.

First we need to verify if, and in which concentration, G-CSF reached the Schwann cells, dorsal root ganglion neurons and motoneurons of the studied nerves after subcutaneous injection. Direct measurement of G-CSF in the peripheral nerve would be the most accurate approach to define its passage over the blood-nerve barrier and measure the concentration at the target tissue. However, direct measurements of G-CSF in peripheral nerve lysates, anterior spinal cord or dorsal root ganglia were not performed in this study because of the high cost of such analysis. We delivered indirect proof of the systemic and dose-related activity of G-CSF in the blood by analyzing the white blood cell count, which was elevated in a dose-dependent way. Measurement of a dose-dependent elevated spleen and liver weight contributed to the proof of systemic G-CSF activity since these organs are known to enlarge due to extramedullary hematopoiesis (Welte et al.,1996).

It is possible that the final G-CSF concentration at the nerve level was insufficient to mimic the observed in vitro effects. The three different doses of G-CSF were based on studies in the CNS (see below). A higher dose of G-CSF may be required, but it has to be kept in mind that 100µg/kg is the maximum accepted dose for humans regarding safety and adverse effects on the long term.

Second, we need to consider if the animal model for CMT1A was adequate. The PMP22<sup>+++</sup> rat has been confirmed to be a reliable model that mimics the clinical situation in human CMT1A patients well, as described in previous work (Sereda et al., 1996, 2003; Grandis et al., 2004; Fledrich et al., 2012). The electrophysiological and histological hallmarks of CMT1A were present in the PMP 22<sup>+++</sup> transgenic animals in our study at the early age of 4 weeks. We observed a three times lower mean sciatic NCV in transgenic rats compared to wild-type controls (4.0 vs 14.0 m/s) and a significant decreased proximal CMAP (0.22 vs 0.76 mV). Grandis et al. described comparable NCVs (5.2 m/s) in the CMT1A rat at 4 weeks of age, yet their measurements in wild-type animals were more than twice as high compared to our study (34.4 m/s). This difference may be attributed to the fact that we performed our electrophysiological analysis on tail nerves, while Grandis et al. used the sciatic nerve. At the histological level, we found no difference in total axon count or fiber density of the sciatic nerve between transgenic and wild-type animals, which is in line with the observations of Grandis et al. in animals < 8 weeks. We observed axonal loss in the tibial nerves of our PMP 22<sup>+++</sup> rats compared to wild-types (“axon density”, resp.  $51.5 \pm 6.05$  vs.  $59.6 \pm 3.67 \times 10^2/\text{mm}^2$ ), but found no data on the axon number in tibial nerves of young rats in literature to compare this result with. Clinical signs of distal muscle involvement (plantar muscle weakness), suggesting axonal degeneration, are reported in the study of Grandis et al. Signs of demyelination were observed in the form of an increased number of demyelinated axons in sciatic and tibial nerves, and increased G-ratio in sciatic but not in tibial nerves. We found resp. 10% and 7% demyelinated axons in sciatic and tibial nerves of transgenic animals and 3% resp. 1% in wild-types. These findings are comparable with the observations of Sereda et al. in eight week-old PMP22<sup>+++</sup> rats, who found demyelination but also axonal loss in sciatic nerves (Sereda et al., 2003). They also noticed less demyelination in the tibial nerve compared to the sciatic nerve, but observed no demyelination at all in wild-types. The difference in age (four versus eight weeks) or an inter-observer variability in analysis of myelination (manual counting) might explain the latter dissimilarity. We did not observe onion bulbs in sciatic or tibial nerve sections, which occurs only from 2.5 months of age according to the study of Sereda et al. Grandis et al. also rarely encountered onion bulbs in sections from 4 week old PMP22<sup>+++</sup> rats.

Taken together, our data confirmed that the animal model provides sufficient electrophysiological and histological features of CMT1A making it an appropriate disease model. Nevertheless, the study could have benefited from clinical and histological hallmarks that can be noticed only in older animals.

The third and probably most important question is if fourteen days of G-CSF therapy are long enough to induce noticeable changes in histology and electrophysiology in our animal model. Since G-CSF pharmacology, to our knowledge, has not been studied before in the PNS at the time that our animal experiments were conducted, the only studies that were available to answer this question were G-CSF (subcutaneous delivered) studies conducted in CNS disorders such as stroke, Alzheimer's and Parkinson's disease.

Several stroke studies in murine models noticed improvement of diverse study outcomes after short subcutaneous G-CSF administration dosed 10 to 100  $\mu\text{g}/\text{kg}$ , for example one day (Gibson et al., 2005; Sehara et al., 2007; Six et al., 2003; Solaroglu et al., 2006, 2009) or two to five days (Shyu et al., 2004; Yanqing et al., 2006; Taguchi et al., 2007). Nevertheless, stroke is an acute event characterized by different pathophysiological processes attacking previously healthy neurons. Regenerative mechanisms play a major role in outcome concerning the attached neurons and their supporting cells in the CNS. On the other hand, CMT1A is a slowly progressive degenerative disease in which the Schwann cells are constitutively affected. Regenerative stimulation may therefore be hindered by their primary dysfunction or may require a longer time of treatment.

Neurodegenerative diseases like Parkinson's disease, Alzheimer's disease or amyotrophic lateral sclerosis (ALS) might serve as better models for study comparison, but have rarely been studied in terms of G-CSF. In different mouse models for Parkinson's disease, beneficial effects on dopaminergic neurons were seen after daily administration of 40  $\mu\text{g}/\text{kg}$  G-CSF subcutaneous for 13 days (Meurer et al., 2006) and 200  $\mu\text{g}/\text{kg}$  for seven days (Cao et al., 2006). Injection of 50  $\mu\text{g}/\text{kg}$  subcutaneous in two mouse models for Alzheimer's disease also resulted in functional and biochemical signs of improvement (Tsai et al., 2007). In two mouse model studies for ALS and one for spinal cord injury, the ways of G-CSF administration were either via an intrathecal pump or carrier virus, making them incomparable.

Knowing that short periods of subcutaneous G-CSF administration can cause noticeable effects in the CNS, the same dosage may by deduction be sufficient in the PNS provided that the G-CSF concentration at the nerve level and the mechanism of action in the CNS would be comparable in the PNS.

This brings us to the question which pathophysiological mechanism could be responsible for a G-CSF effect in the PNS. In the introduction we mentioned the neuroprotective properties of G-CSF in the CNS, that take place by a direct anti-apoptotic and proliferative effect on neurons, as well as by an indirect effect by mobilizing neuroprogenitor stem cells from the bone marrow. The studies that have been conducted in this domain involved a broad range of neurological disorders and shared that the common site of G-CSF action is thought to be on the neuron itself and not the surrounding microglia. Receptor activation was shown to occur specifically in adult neurons and neural progenitor cells (Schneider et al., 2005). In CMT1A, the primary pathophysiological feature is not a neuron pathology; but a slowly progressive Schwann cell pathology that leads in later stages of the disease to axonal degeneration. Our pilot study was based on the finding of a G-CSF receptor on cultured rat primary Schwann cells in vitro with proliferative and anti-apoptotic effects. We suggested that the Schwann cell would be site of G-CSF action (Kleffner et al. 2011, unpublished results) in case of a benefit in early CMT1A, a finding that has been confirmed nor studied in other research projects so far. If we had aimed to study proliferative and anti-apoptotic effects of G-SCF on other sites of action; more particularly motoneurons and dorsal root ganglion neurons, a much longer time of evaluation should have to be applied that encompasses the propagated disease stage with axonal loss. Finally, the translation of the in vitro results into a living animal is not straightforward, and we already mentioned the prerequisite of a proper nerve penetration by G-CSF with this regard.

In conclusion, we have to omit that the study design raises important concerns regarding the length of therapy and disease stage of the animal model; that cannot allow us to draw definite conclusions on the potential effects of G-CSF in CMT pathology.

## **G-CSF and the immune response**

Next to the anti-apoptotic and proliferative effect on neurons and the mobilizing stimulus on neuroprogenitor stem cells, G-CSF is thought to induce a beneficial effect in CNS disease by regulation of local immune responses and stimulation of angiogenesis. (Schneider et al., 2005). Since local inflammation contributes to the pathogenesis and progression of CMT, it seemed opportune to investigate the effect of G-CSF on PNS inflammation (Maurer et al. 2002, Groh et al. 2012).

In a mouse model for CMT, demyelination was accompanied by peri-axonal infiltration of macrophages and T-lymphocytes, in order to remove myelin by phagocytosis (Maurer et al. 2002). Pro-inflammatory changes may play a role in other CNS and PNS disease. In an animal study for ALS, for example, G-CSF was shown to reduce inflammation both in the CNS and PNS. An increase of the availability of anti-inflammatory monocytes was observed, thereby delaying disease progression (Polari et al., 2011). We investigated the presence of macrophages, T-lymphocytes and granulocytes in distal sciatic nerve sections and compared both transgenic and wild-type animals for a possible effect of G-CSF. We were not able to confirm the findings of Maurer et al. in our rat model. It has to be taken in consideration that our observations were made at the early age of four weeks, whereas the observations by Maurer and colleagues were made in animals aged over two months (Maurer et al. 2002). Although a trend towards more macrophages was seen with the 100 µg G-CSF doses, this was statistically not significant ( $p=0.2$ ). This insignificant result may be influenced by the small sample size (16 animals) that was available for immunohistochemical analysis. To make general conclusions, the intervention should be repeated in a larger sample.

Some question marks about the role of the immune response in CMT and the actions of G-CSF have to be postulated with this regard. First, there is a high amount of cross-talk as a typical hallmark of regulatory factors of the immune system that also may apply to G-CSF, making its action in local immune responses unpredictable (Roberts et al., 2005; Anderlini et al., 2012). This may explain why G-CSF is reported to have both pro- and anti-inflammatory effects depending on the clinical setting (Weis et al., 1999; Hartung, 1998). Furthermore, multiple factors can influence G-CSF action directly or indirectly in vivo, and adaptive mechanisms may functionally interfere with its effect. One interfering factor could be downregulation of the G-CSF-R, which was described in bone marrow cells after endogenous elevation of G-CSF (Demetri et al., 1991; Avalos, 1996).

Several models for nerve injury on the other hand, suggest receptor upregulation at the neuronal level (Pitzer et al., 2010). In conclusion, it remains unclear what the specific role of G-CSF is in CNS or PNS inflammation.

### **G-CSF and angiogenesis**

Several studies on experimental stroke documented the stimulatory effect of G-CSF on angiogenesis (Schneider et al. 2005; Lee et al., 2005; Bussolino et al, 1991). We were interested in studying the effect of G-CSF on angiogenesis in the PNS. G-CSF has a local proliferative influence on mature endothelial cells and mobilizes endothelial progenitor cells from the bone marrow (Körbling et al.,2006). Although the number of blood vessels appeared to be higher among transgenic animals receiving 100 µg/kg G-CSF, this finding was not statistically significant. We made our observation in a small number of animals. Extended animal numbers and observation time may be required to observe a significant difference. The therapeutic relevance of these findings and considerations requires further investigation.

### **At least some new findings**

Let's discuss two interesting findings of this study that have not been described previously in CMT1A. We noticed a significant enlarged nerve area and an elevated blood vessel number (on manual count) in the sciatic nerve of our PMP22<sup>+/+</sup> transgenic rats compared to wild-types. The interpretation of these features came out to be a challenge. We mentioned the study of Mauer et al. in which demyelination was accompanied by peri-axonal infiltration of macrophages and T-lymphocytes in a mouse model for CMT (Maurer et al., 2002). We could pose that a local inflammatory response in CMT may result in enlargement of the nerve diameter and enhance angiogenesis, which would indeed explain both features. We could not find significant differences in the endoneural presence of immune cells in transgenic animals compared to placebo, regardless of G-CSF treatment, so that this proposed mechanism could not be proven in our study. Nevertheless, due to the small sample size that was available for immunohistochemical analysis (10 transgenic and 6 wild type animals), this does not mean that the observations of Mauer and colleagues are invalid. The increase in endoneural blood vessels could in part account for the observed increased nerve area. The pathophysiology of the latter finding is unsure. It is known that local inflammation in the CNS may provide a

stimulus for neo-vascularization by the release of vascular growth factors, like vascular endothelium derived growth factor (VEGF) (Carmeliet, 2003). VEGF is a potent stimulator of survival and proliferation of endothelium, and can induce a similar response in adult neurons, astroglia and Schwann cells who also express functional VEGF receptors (Sondell et al., 1999). The Schwann cell on the other hand, is known to secrete VEGF during embryogenesis to direct vascularization along the nerve path (Zacchigna et al., 2008). Interestingly, VEGF can also be induced by G-CSF (Anderlini et al., 2012). In vivo and in vitro studies merged that VEGF has pleiotropic activity in the nervous system, including neurogenesis, neuronal migration, survival of multiple adult axons types and axon guidance after injury (for review see Zacchigna et al., 2008; Mackenzie et al., 2012). In a rat model for diabetic neuropathy, one study documented upregulation of VEGF in Schwann cells and neurons upon functional alterations in the peripheral nerves (Samii et al., 1999). We pose the theoretical hypothesis that the demyelination and possibly local inflammation in the peripheral nerve in CMT1A might trigger release of VEGF from Schwann cells or other supportive cells, leading to increased vascularization. Again, this study did not investigate this theoretical mechanism of action.

### **G-CSF for CMT: end of story?**

Finally, some remarks have to be made regarding a hypothetical use of G-CSF for CMT patients. Because of the disease's chronic nature, CMT patients should preferably be offered a lifelong therapy that is safe on the short and long term. It should be easy to administer and have a low adverse drug response profile in the light of the mild and slowly progressive symptoms of CMT.

On the short term, G-CSF has been proven to be safe and has minor adverse reactions, with leukocytosis and bone pain being the most frequent side-effects. The effect of chronic leukocytosis, however, is insufficiently studied in humans. Splenomegaly and risk of spleen rupture is possible with chronic use (Anderlini et al., 2002). Some concerns are postulated in literature regarding the safety of G-CSF in the development of malignancy. Two randomized clinical trials in more than 5000 healthy subjects showed no significant relation to malignancy, but the follow up-period was short (for review see Beekman et al; 2012).

On the long term, the risk of a myelodysplastic syndrome (MDS) development remains unclear and there is a suspicion of elevated MDS prevalence when G-CSF is given to patients with breast cancer.

Next to this concern, the route of G-CSF administration is less favorable. It is given parenteral because of gastrointestinal break down, and because of the short plasma half life ( $t_{1/2} = 4$  hours), some authors recommend a continuous mode of delivery in chronic settings by either a subcutaneous pump (Pitzer et al., 2010) or viral carrier (Henriques et al., 2010). This makes G-CSF less attractive for chronic daily use.

## Conclusions and perspectives for further research

This research project was designed as a pilot study to examine the short-term effects of G-CSF on peripheral nerve myelination, axonal containment and vascularization in a rat model for CMT1A. Our findings did not support the beneficial effect of G-CSF on CMT1A rat Schwann cells that was seen in the in-vitro observations at an electrophysiological or histological level. A longer period of treatment may be required to show beneficial effects of G-CSF. Nerve regeneration is a slow process after all, and an evaluation period of two months or more better parallels the mechanisms of de- and re-myelination in CMT1A. This would allow to evaluate the effects on clinical symptoms seen at this disease stage in muscle strength, gait and balance of the animal model. Since a dose of 100 µg/kg G-CSF given for longer than 13 weeks is known to cause hind-leg problems in the healthy rat model due to peri-articular swelling (Zsebo et al., 1986), testing of forelimbs would be recommended to avoid any interference.

This study made some unique electrophysiological and histological observations in the PMP22<sup>+/+</sup> rat at four weeks and observed some interesting new features concerning the peripheral nerve vascularization of CMT1A rats which may serve as a basis for future research. The unexpected finding of enlarged nerve area and extended vascularization in PMP22 transgenic rats demands further study. More sensitive methods to detect vascularization and, above all, a larger sample size are required in order to accurately investigate and quantify this feature, like analysis of endothelium with different markers or 3D-reconstructions of blood vessels to explore branching. Furthermore, ensuing research should be done to identify the mechanisms involved in vascularization of diseased and healthy nerves (Carmeliet et al., 2003). The role of G-CSF and other hematopoietic growth factors in neuroprotection and regeneration has been established in experimental models in the CNS and the PNS. Further research will be necessary to evaluate the role of hematopoietic growth factors in the PNS. The pathophysiology and impact of local inflammation in degenerative neuropathies also requires further investigation (Maurer et al., 2002; Fledrich et al., 2012). It is our hope that better insight in these domains might open windows for further therapeutic strategies.

Despite extensive research during the past decades, there is to date no causal therapy for any subtype of the CMT family (Young et al., 2008; Fledrich et al., 2012). Therapeutic strategies

should be based on the underlying disease mechanism. Pathophysiological studies demonstrated several signal transduction pathways that are involved in myelination and are disrupted in CMT. Further insight into the molecular pathophysiology of these pathways may provide new strategies for therapy. From this point of view, therapies that repair or modify the PMP22 duplication or alter its mRNA transcripts to achieve a balanced control of PMP22 expression seem the most promising findings for the treatment of CMT1A. Both vitamin C and progesterone antagonist Onapriston reduced the toxic overexpression of PMP22 mRNA in murine models for CMT1A. Nevertheless, these effects could not be established in humans so far. Caution should be taken when pharmacologically lowering the PMP22 gene expression, because too little expression can cause neuropathy with liability to pressure palsies (HNPP) (Fledrich et al., 2012). Research on this domain is ongoing and currently focuses on the use of viral vectors and siRNA in PMP22 gene modulation. Another strategy, in line with the scope of this study, is to identify substances that support axon containment. This is relevant for CMT, as the axonal degeneration is the direct cause of clinical manifestations rather than the demyelination. The neurotrophic factor Neurothrophin 3 was proven to favor axonal regeneration and sensory loss in a small clinical pilot study (Sahenk et al., 2005), but these findings have to date not been confirmed. Finally, drugs that restore misfolded proteins or target their overload of the cell's degradation pathways are a last therapeutic target under study in CMT animal models (Khajavi et al., 2007). They might be promising for distinct subtypes of CMT.

We hope that our study may contribute as an aid and inspiration to develop future therapeutic strategies for CMT.

## References

1. Anderlini P, Champlin R. Use of Filgrastim for stem cell mobilization and transplantation in high-dose cancer chemotherapy. *Drugs* 2002; 62(sup11):79-88.
2. Anderlini P, Champlin RE. Biologic and molecular effects of granulocyte colony-stimulating factor in healthy individuals: recent findings and current challenges. *Blood* 2008; 111(4):1767-72.
3. Avalos BR. Molecular analysis of the granulocyte colony-stimulating factor receptor. *Blood* 1996; 88:761-77.
4. Bath PMW, Sprigg N. Colony stimulating factors (including erythropoietin, granulocyte colony stimulating factor and analogues) for stroke. *Cochrane Database of Systematic Reviews* 2007, Issue 2. Art. No.: CD005207. DOI: 10.1002/14651858.CD005207.pub3.
5. Beekman R, Touw IP. G-CSF and its receptor in myeloid malignancy. *Blood* 2010; 115(25):5131-36.
6. Buddhala C, Prentice H, Wu JY. Models of action of taurine and granulocyte colony-stimulating factor in neuroprotection. *J Exp Clin Med* 2012; 4(1):1-7.
7. Burns J, Ouvrier RA, Yiu EM, Joseph PD, Kornberg AJ, Fahey MC, Ryan MM. Ascorbic acid for Charcot-Marie-Tooth disease type 1A in children: a randomised, double-blind, placebo-controlled, safety and efficacy trial. *Lancet Neurol.* 2009 Jun;8(6):537-44.
8. Bussolino F, Wang JM, Defilippi P et al. Granulocyte- and granulocyte-macrophage-colony stimulating factors induce human endothelial cells to migrate and proliferate. *Nature* 1989; 337:471-73.
9. Cao XQ, Arai H, Ren YR, Oizumi H, Zhang N, Seike S, Furuya T, Yasuda T, Mizuno Y, Mochizuki H. Recombinant human granulocyte colony-stimulating factor protects against MPTP-induced dopaminergic cell death in mice by altering Bcl-2/Bax expression levels. *J Neurochem.* 2006 Nov; 99(3):861-7.
10. Carmeliet P. Angiogenesis in health and disease. *Nature Med* 2003; 9:653-60.
11. Carenini S, Maurer M, Werner A, Blazyca H, Toyka KV, Schmid CD et al. The role of macrophages in demyelinating peripheral nervous system of mice heterozygously deficient in P0. *J Cell Biol* 2001; 152:301–308.

12. Chiò A, Mora G, La Bella V et al. Repeated courses of granulocyte colony-stimulating factor in amyotrophic lateral sclerosis: clinical and biological results from a prospective multicenter study. *Muscle Nerve*. 2011 Feb;43(2):189-95. doi: 10.1002/mus.21851
13. Demetri GD, Griffin JD. Granulocyte colony-stimulating factor and its receptor. *Blood* 1991; 78:2791-2808.
14. Diederich K, Schäbitz WR, Minnerup J. Seeing old friends from a different angle: Novel properties of hematopoietic growth factors in the healthy and diseased brain. *Hippocampus*. 2012; 22(5):1051-57.
15. England TJ, Gibson CL, Bath PM. Granulocyte-colony stimulating factor in experimental stroke and its effects on infarct size and functional outcome: a systematic review. *Brain Res Rev* 2009; 62(1):71-82.
16. Fledrich R, Stassart R, Sereda M. Murine therapeutic models for Charcot Marie Tooth disease. *British Medical Bulletin* 2012;1–25.
17. Gibson CL, Bath PM, Murphy SP. G-CSF reduces infarct volume and improves functional recovery after transient focal cerebral ischemia in mice. *J Cereb Blood Flow Metab* 2005; 25:431-9.
18. Grandis M, Leandri M, Vigo T et al. Early abnormalities in sciatic nerve function and structure in a rat model of Charcot-Marie-Tooth type 1A disease. *Experimental Neurology* 2004;190:213– 223.
19. Groh J, Weis J, Zieger H, Stanley R, Heuer H, Martini R. Colony-stimulating factor 1 mediates macrophage-related neural damage in a model for Charcot-Marie-Tooth disease type 1X. *Brain* 2012; 135:88-104.
20. Guenard V, Montag d, Schachner M, Martini R. Onion bulb cells in mice deficient for myelin genes share molecular properties with immature, differentiated non-myelinating and denervated schwann cells. *Glia* 1996; 18(1):27-38.
21. Hartung T. Anti-inflammatory effects of granulocyte colony stimulating factor. *Curr Opin Hematol* 1998;5:221-5.
22. Hattori N, Yamamoto M, Yoshihara T et al. Demyelinating and axonal features of Charcot-Marie-Tooth disease with mutations of myelin-related proteins (PMP22, MPZ and Cx32): a clinicopathological study of 205 Japanese patients. *Brain* 2003; 126:134-151.

23. Henriques A, Pitzer C, Dittgen T. CNS-targeted Viral Delivery of G-CSF in an Animal Model for ALS: Improved Efficacy and Preservation of the Neuromuscular Unit. *Mol Ther.* 2010 Dec 7. 19(2): 284–92.
24. Kamholz J, Menichella D, Jani A et al. Charcot-Marie-Tooth disease type 1. Molecular pathogenesis to gene therapy. *Brain* 2000; 123:222-33
25. Khajavi M, Shiga K, Wiszniewski W, et al. Oral curcumin mitigates the clinical and neuropathologic phenotype of the Trembler-J mouse: a potential therapy for inherited neuropathy. *Am J Hum Genet* 2007; 81: 438–53.
26. Kirsch F, Krüger C, Schneider A. The receptor for granulocyte-colony stimulating factor (G-CSF) is expressed in radial glia during development of the nervous system. *BMC Dev Biol.* 2008; 27:8-32.
27. Klein CJ. The inherited neuropathies. *Neurol Clin* 2007; 25:173–207.
28. Körbling M, Reuben JM, Gao H et al. Recombinant human granulocyte-colony-stimulating factor –mobilized and apheresis-collected endothelial progenitor cells: a novel blood cell component for therapeutic vasculogenesis. *Transfusion* 2006; 46(10):1795-1802.
29. Lee ST, Chu K, Jung KJ et al. Granulocyte colony-stimulating factor enhances angiogenesis after focal cerebral ischemia. *Brain Research* 2005; 1058:120-128.
30. Lupski J, de Oca-Luna R, Slaugenhaupt S, et al. DNA duplication associated with Charcot-Marie-Tooth disease type 1A. *Cell* 1991;66(2):219-32.
31. Mackenzie F, Ruhrberg C. Diverse roles for VEGF-A in the nervous system. *Development* 2012; 139: 1371-80.
32. Martyn CN, Hughes RAC. Epidemiology of peripheral neuropathy. *J Neurol Neurosurg Psychiatry* 1997; 62: 310-18.
33. Mäurer M, Kobsar I, Berghoff M, Schmid CD, Carenini S, Martini R. Role of immune cells in animal models for inherited neuropathies: facts and visions. *J Anat* 2002;200:205-414.
34. McCollum M, Ma Z, Cohen E, Leon R, Tao R, Wu JY, Maharaj D, Wei J. Post-MPTP treatment with granulocyte colony-stimulating factor improves nigrostriatal function in the mouse model of Parkinson's disease. *Mol Neurobiol.* 2010 Jun;41(2-3):410-19.
35. Meuer K, Pitzer C, Teismann P et al. Granulocyte-colony stimulating factor is neuroprotective in a model of Parkinson's disease. *J Neurochem* 2006; 97:675–86.

36. Meyer zu Horste G, Prukop T, Liebetanz D, Mobius W, Nave KA, Sereda MW. Antiprogestosterone therapy uncouples axonal loss from demyelination in a transgenic rat model of CMT1A neuropathy. *Ann Neurol* 2007; 61: 61–72.
37. Micallef J, Attarian S, Dubourg O. Effect of ascorbic acid in patients with Charcot–Marie–Tooth disease type 1A: a multicentre, randomised, double-blind, placebo-controlled trial. *Lancet Neurol*. 2009;8:1103–1110.
38. Pareyson D, Marchesi C. Diagnosis, natural history, and management of Charcot-Marie-Tooth disease. *Lancet neurol* 2009, 8(7):654 -67.
39. Pareyson D, Reilly MM, Schenone A et al. Ascorbic acid in Charcot-Marie-Tooth disease type 1A (CMT-TRIAAL and CMT-TRAUK): a double-blind randomised trial. *Lancet neurol* 2011;10(4):320-8.
40. Passage, E., J. C. Norreel, et al. (2004). "Ascorbic acid treatment corrects the phenotype of a mouse model of Charcot-Marie-Tooth disease." *Nat Med* 10(4): 396-401.
41. Pitzer C, Klussmann S, Krüger C et al. The hematopoietic factor granulocyte-colony stimulating factor improves outcome in experimental spinal cord injury. *J Neurochem* 2010; 113:930–42.
42. Pitzer C, Krüger C, Plaas C, Kirsch F et al. Granulocyte-colony stimulating factor improves outcome in a mouse model of amyotrophic lateral sclerosis. *Brain*. 2008 Dec;131(12):3335-47.
43. PJ Dyck, PK Thomas (Eds.), *Peripheral neuropathy* (4th ed.), Elsevier Saunders, Philadelphia (2005), pp. 1623-58.
44. Pollari E, Savchenko E, Jaronen M et al. Granulocyte colony stimulating factor attenuates inflammation in a mouse model of amyotrophic lateral sclerosis. *J Neuroinflammation*. 2011; 8: 74.
45. Roberts AW. G-CSF: a key regulator of neutrophil production, but that's not all! *Growth Factors* 2005, 23(1):33-41.
46. Sahenk Z, Nagaraja HN, Mc Cracken BS et al. NT-3 promotes nerve regeneration and sensory improvement in CMT1A mouse models and in patients. *Neurology* 2005;65(5):681-9.
47. Samii A, Unger J, Lange W: Vascular endothelial growth factor expression in peripheral nerves and dorsal root ganglia in diabetic neuropathy in rats. *Neurosci Lett* 1999;262:159–162.

48. Sanchez-Ramos J, Song S, Sava V et al. Granulocyte colony stimulating factor decreases brain amyloid burden and reverses cognitive impairment in Alzheimer's mice. *Neurosci.* 2009 Sep 29;163(1):55-72.
49. Schäbitz WR, Kollmar R, Schwaninger M et al. Neuroprotective effect of granulocyte colony-stimulating factor after focal cerebral ischemia. *Stroke* 2003; 34:745-54.
50. Schneider A, Kruger C, Steigleder T et al. The hematopoietic factor G-CSF is a neuronal ligand that counteracts programmed cell death and drives neurogenesis. *J Clin Invest* 2005;115(8): 2083-98.
51. Sereda M, Griffiths I, Pühlhofer A, Stewart H, Rossner MJ, Zimmerman F, Magyar JP, Schneider A, Hund E, Meinck HM, Suter U, Nave KA. A transgenic rat model of Charcot-Marie-Tooth disease. *Neuron.* 1996 May;16(5):1049-60.
52. Sereda MW, Meyer zu Horste G, Suter U, Uzma N, Nave KA. Therapeutic administration of progesterone antagonist in a model of Charcot–Marie–Tooth disease (CMT1A). *Nat Med* 2003; 9: 1533–37.
53. Shyu WC, Lin SZ, Yang HI et al. Functional recovery of stroke rats induced by granulocyte-colony-stimulating factor- stimulated stem cells. *Circulation* 2004; 110:1857-54.
54. Singh S. From exotic spice to modern drug? *Cell* 2007; 130: 765–68.
55. Six I, Gasan G, Mura E, Bordet R. Beneficial effect of pharmacological mobilization of bone marrow in experimental cerebral ischemia. *Eur J Pharmacol* 2003; 458:327-8.
56. Sondell M, Lundborg G, Kanje M. Vascular endothelial growth factor has neurotrophic activity and stimulates axonal outgrowth, enhancing cell survival and Schwann cell proliferation in the peripheral nervous system. *J Neurosci* 1999;19:5731–40.
57. Stanley, E.F.. Sensory and motor nerve conduction velocities and the latency of the H reflex during growth of the rat. *Exp Neurol* 1981; 71 (3),497– 506.
58. Suter U, Scherer S. Disease mechanisms in inherited neuropathies. *Nat rev neurosci* 2003(4);9:714-726.
59. Tsai KJ, Tsai YC, Shen CK. G-CSF rescues the memory impairment of animal models of Alzheimer's disease. *J Exp Med.* 2007 Jun 11;204(6):1273-80.
60. Verhamme C, de Haan RJ, Vermeulen M. Oral high dose ascorbic acid treatment for one year in young CMT1A patients: a randomised, double-blind, placebo-controlled phase II trial. *BMC Med* 2009 Nov 12;7:70.

61. Welte K, Gabrilove J, Bronchud MH, Platzer E, Morstyn G. Filgrastim (r-metHuG-CSF): The first 10 years. *Blood* 1996;88(6):1907-29.
62. Young P, De Jonghe P, Stögbauer F, Butterfass-Bahloul T. Treatment for Charcot-Marie-Tooth disease. *Cochrane Database Syst Rev*. 2008 Jan 23;(1):CD006052.
63. Zacchigna S, Lambrechts D, Carmeliet P. Neurovascular signaling defects in neurodegeneration. *Nat Rev Neurosci* 2008; 9:169-181.
64. Zhao C, Xie Z, Wang P et al. Granulocyte-colony stimulating factor protects memory impairment in the senescence-accelerated mouse (SAM)-P10. *Neurol Res*. 2011 May;33(4):354-59.
65. Zsebo KM, Cohen AM, Murdock DC, et al. Recombinant human granulocyte colony stimulating factor: Molecular and biological characterization. *Immunobiol*. 1986;172:175-184.

# Curriculum Vitae

